

Review

# Metabolomics Approach to Reveal the Effects of Ocean Acidification on the Toxicity of Harmful Microalgae: A Review of the Literature

Tsz-Ki Victoria Tsui<sup>1</sup> and Hang-Kin Kong<sup>2,3,\*</sup>

<sup>1</sup> Department of Applied Biology and Chemical Technology, The Hong Kong Polytechnic University, Hung Hom, Kowloon, Hong Kong

<sup>2</sup> Department of Food Science and Nutrition, The Hong Kong Polytechnic University, Hung Hom, Kowloon, Hong Kong

<sup>3</sup> Research Institute for Future Food, The Hong Kong Polytechnic University, Hung Hom, Kowloon, Hong Kong

\* Correspondence: hang-kin.kong@polyu.edu.hk; Tel.: +852-3400-8708

**Abstract:** Climate change has been associated with intensified harmful algal blooms (HABs). Some harmful microalgae produce toxins that accumulate in food webs, adversely affecting the environment, public health and economy. Ocean acidification (OA) is a major consequence of high anthropogenic CO<sub>2</sub> emissions. The carbon chemistry and pH of aquatic ecosystems have been significantly altered as a result. The impacts of climate change on the metabolisms of microalgae, especially toxin biosynthesis, remain largely unknown. This hinders the optimization of HAB mitigation for changed climate conditions. To bridge this knowledge gap, previous studies on the effects of ocean acidification on toxin biosynthesis in microalgae were reviewed. There was no solid conclusion for the toxicity change of saxitoxin-producing dinoflagellates from the genus *Alexandrium* after high CO<sub>2</sub> treatment. Increased domoic acid content was observed in the diatom *Pseudo-nitzschia*. The brevetoxin content of *Karenia brevis* remained largely unchanged. The underlying regulatory mechanisms that account for the different toxicity levels observed have not been elucidated. Metabolic flux analysis is useful for investigating the carbon allocations of toxic microalgae under OA and revealing related metabolic pathways for toxin biosynthesis. Gaining knowledge of the responses of microalgae in high CO<sub>2</sub> conditions will allow the better risk assessment of HABs in the future.

**Keywords:** ocean acidification; marine microalgal toxin; harmful algal bloom; metabolic flux analysis



**Citation:** Tsui, T.-K.V.; Kong, H.-K. Metabolomics Approach to Reveal the Effects of Ocean Acidification on the Toxicity of Harmful Microalgae: A Review of the Literature.

*AppliedChem* **2023**, *3*, 169–195.

<https://doi.org/10.3390/appliedchem3010012>

Academic Editors: Theodoros

Chatzimitakos and

Athanasia Kasouni

Received: 13 February 2023

Revised: 2 March 2023

Accepted: 7 March 2023

Published: 16 March 2023



**Copyright:** © 2023 by the authors. Licensee MDPI, Basel, Switzerland. This article is an open access article distributed under the terms and conditions of the Creative Commons Attribution (CC BY) license (<https://creativecommons.org/licenses/by/4.0/>).

## 1. Introduction

Harmful algal blooms (HABs) refer to the rapid growth of phytoplankton, including cyanobacteria, dinoflagellates, raphidophytes, haptophytes, and macroalgae, which exerts harmful effects on the environment, human health, and the economy [1]. High microalgal biomass accumulation during HABs can cause hypoxia, suffocating surrounding aquatic organisms [2]. Some HAB species can produce algal toxins that accumulate in aquatic food webs [3]. Apart from causing the massive death of marine mammals and fish [4], algal toxins can lead to intoxication in humans. Approximately 50,000 to 500,000 cases of intoxication with a 1.5% mortality rate have been reported annually due to the consumption of contaminated shellfish or fish [5]. The health costs associated with HABs are substantial, ranging from around USD 90 to USD 12,000 for digestive and respiratory illnesses with different severities [6]. The aquacultural industry is the most vulnerable when considering the direct economic losses caused by HABs. From the 1980s to the 2010s, the aquacultural industry in Korea lost a total of USD 121 million due to HAB-induced fish and shellfish deaths [7]. In addition to the aquacultural industry, tourism is adversely affected by HABs. It was reported that the monthly revenue of coastal lodgings and restaurants decreased

by USD 2.8 and 3.7 million, respectively, in Fort Walton Beach and Destin in Florida when HABs occurred [8]. To mitigate the negative effects of HABs, costly monitoring programs and mitigation measures are conducted in different regions, such as the US, Europe, and Australia, as well as by intergovernmental organizations [9].

The direct link between HABs and climate change was first affirmed in the Special Report on the Ocean and Cryosphere in a Changing Climate, published by the Intergovernmental Panel on Climate Change in 2019 [1]. Climate change has profoundly changed the aquatic environment over the years by increasing the surface temperature, acidifying water bodies, shifting nutrient availability, altering salinity, etc. Several studies have reviewed the association between climate change and intensified HABs [10–13]. In parallel with the spatial expansions and frequencies of HABs, the frequency and distribution of human intoxication by algal toxins have also increased globally [4]. According to the Harmful Algae Event Database (HAEDAT), 1598 HAB-related seafood poisoning cases were reported during the 20th century. A nearly five-fold increase in the number of cases (7843) was observed from 2001 to 2022. Intensified HABs can also further alter the food webs and disturb the ecosystem. The physiology, mortality, and toxicity of marine organisms at higher trophic levels were found to have changed when co-exposed to algal toxins and climate change stressors, as summarized by Griffith and Gobler [14]. Given the above-mentioned scenario, it is believed that the adverse effects of HABs will be aggravated in the future.

## 2. Algal Toxins

Intensified HABs of toxic microalgae may increase the algal toxins in aquacultures, subsequently raising the risks of seafood poisoning [15]. Consumption of contaminated seafood can lead to different poisoning syndromes, depending on the types of algal toxins accumulated in shellfish during HABs. As of December 2019, the incidence of paralytic shellfish poisoning (PSP) and diarrhetic shellfish poisoning (DSP) accounted for approximately one third of the reported cases of human intoxication, with PSP contributing 35% and DSP contributing 30% [16]. According to the data, the incidence of amnesic shellfish poisoning (ASP) was relatively low, at 9%, whereas both neurotoxic shellfish poisoning (NSP) and azaspiracid shellfish poisoning (AZP) each accounted for only 1% of cases.

### 2.1. Paralytic Shellfish Poisoning

The causative agents of PSP, saxitoxin (STX) and its 57 analogues, are collectively known as paralytic shellfish toxins (PSTs) [17]. STX is composed of a tricyclic 3,4-propinoperhydro-purine backbone with two guanidine groups [18]. The analogues have been classified into different groups according to the side group moieties. PSTs are mainly produced by eukaryotic marine dinoflagellates from the genera *Alexandrium*, *Gymnodinium*, and *Pyrodinium* [19,20]. Prokaryotic freshwater cyanobacteria from the genera *Anabaena*, *Cylindrospermopsis*, *Aphanizomenon*, *Planktothrix*, and *Lyngbya* are producers of PSTs as well [21–24]. The toxicity levels of these analogues vary depending on the structures. Generally, the toxicity levels of STXs are inversely proportional to the degree of sulfation [17]. PSTs selectively and reversibly bind to receptor site 1 of the voltage-gated sodium channels in the nerves and muscles [25]. Due to the blockage of the channels, the propagation of action potential is terminated, leading to symptoms such as paralysis, burning sensations, and numbness [26]. In serious cases, death can result due to respiratory failure [27]. Most reported PSP cases were contributed by the toxic *Alexandrium* species, which are mainly present in Northern Europe, the Mediterranean, Northern Asia, East Asia, and North America [28–31]. Recently, the geographical distribution of *Alexandrium* has been expanded towards the poles [32].

### 2.2. Diarrhetic Shellfish Poisoning

Okadaic acid and its derivatives, the dinophysistoxins (DTXs), are lipophilic polyketides predominately produced by toxic dinoflagellates from the genera *Prorocentrum* and *Dynophysis* [33]. For human adults, DSP symptoms occur when a minimum dosage of 40 µg okadaic acid equivalents is consumed [34]. According to the Food and Agriculture

Organization (FAO), the recommended okadaic equivalents for okadaic acid, DTX1, and DTX2 are 1.0, 1.0, and 0.5, respectively [35]. Diarrhea, nausea, vomiting, and abdominal pain are the common symptoms of DSP [36]. DSP is generally not life-threatening, and hospitalization is not required [37]. As potent inhibitors of serine/threonine phosphatases [38], okadaic acids show specifically high binding affinity to protein phosphatase 1 (PP1) and protein phosphatase 2 (PP2) [39]. The gastrointestinal symptoms of DSP may be a result of inhibited intestinal PP activities by okadaic acids [40]. In addition, the inhibiting effect of okadaic acids may induce the hyperphosphorylation of proteins that regulate the sodium secretion of intestinal cells [41]. The release of sodium from cells disturbs the osmotic gradient balance and subsequently causes the passive loss of fluids, leading to diarrhea. Both *Prorocentrum* and *Dynophysis* have expanded their niches in recent years. *P. minimum* is the most studied *Prorocentrum* species and is widespread in the Black Sea, the Baltic Sea, Lake Nakanoumi, the Mexican coast, and the Philippines [42]. The expansion of *Dynophysis* was observed in the coastal areas of the United States, Canada, and South Africa [13]. Moreover, increased abundances of *Prorocentrum* and *Dynophysis* in the Northeast Atlantic were reported [43].

### 2.3. Amnesic Shellfish Poisoning

ASP is caused by the consumption of domoic acid (DA)-accumulated shellfish. Red algae such as *Chondria armata* and diatoms from the genera *Pseudo-nitzschia* and *Nitzschia* (*N. navis-varingica* and *N. bizertensis*) are the primary producers of DA [44,45]. DA, a tricarboxylic amino acid, is analogous to glutamic acid and kainic acid [46]. Several DA isomers (isodomic acid A-H, 5' epi-DA) have been identified [47]. With such structural similarity, Das can bind and activate three ionotropic glutamate receptor subtypes (*N*-methyl-D-aspartate (NMDA), kainate, and  $\alpha$ -amino-3-hydroxy-5-methyl-4-isoxazole propionate (AMPA) receptors) located on the dendrites of postsynaptic cells [48,49]. An influx of calcium ions ( $\text{Ca}^{2+}$ ) into neurons is induced upon the activation of kainate and AMPA receptors [50], while an influx of both  $\text{Ca}^{2+}$  and sodium ions ( $\text{Na}^+$ ) is induced upon the activation of the NMDA receptor [51]. Desensitization is prevented by the low conformational mobility of DAs when docked to the receptors, leading to a continuous flow of cations to the postsynaptic cells [52]. DAs exert excitotoxic effects primarily through excess intracellular  $\text{Ca}^{2+}$ , which triggers the mobilization of glutamate-containing vesicles towards the membrane surface, followed by the release of glutamate (Glu) into the synaptic cleft [53]. Excess Glu results in neurodegeneration and apoptosis [54,55]. Since neurons in the hippocampus, where the consolidation of memories takes place, are affected by DAs [56], symptoms such as short-term memory loss and anterograde amnesia may result [57]. Generally, the toxicity of DA isomers is lower than that of DA because of the lower binding affinity of DA isomers to glutamate receptors [58–60]. One of the major DA producers, *Pseudo-nitzschia*, has been detected in the Pacific Ocean and the Southern Ocean [61]. Expanded distributions of *Pseudo-nitzschia* and *N. navis-varingica* have been observed recently [44]. Several locations, including the Arctic, Angola, Singapore, Ukraine, and Pakistan, have recorded the presence of *Pseudo-nitzschia* for the first time, while *N. navis-varingica* has expanded to Malaysia, Australia, Indonesia, and the Philippines.

### 2.4. Neurotoxic Shellfish Poisoning

NSP is caused by the consumption of shellfish contaminated with brevetoxins (PbTx). PbTx are a set of cyclic polyether neurotoxins primarily produced by dinoflagellate *Karenia brevis* [62]. Besides *K. brevis*, recent research indicated PbTx production by raphidophyte *Chattonella* cf. *verruculosa* [63]. PbTx-1 and PbTx-2 are regarded as the parent molecules for other derivatives based on their different structural backbones. The toxicity of all identified natural derivatives is lower than that of the parent molecules [64]. PbTx bind specifically to receptor site five of the voltage-gated sodium channels in the nerves and muscles, with a preference for those located in the nerves [65,66]. The influx of  $\text{Na}^+$  ions into the cells is induced upon the activation of the sodium channels. Prolonged membrane depolarization

persistently initiates the generation of action potentials in nerves and muscles, causing symptoms such as paresthesia, vertigo, and malaise [67]. Blooms of *K. brevis* occur nearly annually along the southwestern coast of Florida, which is notoriously known as the “Florida red tide” [68]. The low incident rate of NSP may be credited to the successful monitoring program of constantly occurring red tides. Apart from Florida, where regular red tides take place, a few large outbreaks of NSP have been reported in New Zealand and North Carolina [69].

### 2.5. Azaspiracid Shellfish Poisoning

Azaspiracids (AZAs) are polyether phytotoxins produced by some dinoflagellate species from the genera *Azadinium* and *Amphidoma* and the causative toxin of AZP [70]. AZA was named based on its unique spiro ring assemblies [71]. To date, over 60 AZA analogues have been identified [72]. They are different in the degrees of methylation and/or the number of hydroxyl groups and carboxyl groups that they possess. However, among the numerous analogues, only AZA1, AZA2, and AZA3 levels are monitored for regulatory purposes [33]. The symptoms of AZP are similar to those of DSP, including diarrhea, vomiting, nausea, and stomach cramps [73]. A minimum dosage ranging from 23 to 86 µg/person of AZA can have observable adverse health effects [74]. Unlike other phytotoxins, the molecular target(s) of AZAs has not been fully understood. Although the blocking of the hERG (human ether-à-go-go related gene) potassium channel by AZA1-3 was demonstrated in a recent study, relatively high concentrations of AZAs were required [75]. Therefore, there may be other molecular targets that have not been identified. The presence of toxigenic *Azadinium* species has been reported worldwide, including in the North Atlantic [76,77], Eastern South Atlantic [78], Mediterranean [79], Western Pacific [80], Eastern North Pacific [81], and Eastern South Pacific [82]. On the other hand, the occurrence of toxigenic *Amphidoma* species was only recorded in the North Atlantic [77,83,84].

## 3. Ocean Acidification

Ocean acidification (OA) is one of the major aspects of climate change and has indeed been significantly influencing the aquatic environment, where toxigenic microalgae live. Carbon dioxide (CO<sub>2</sub>) emissions have increased dramatically since the Industrial Revolution, primarily due to the combustion of fossil fuels. At present, the recorded atmospheric CO<sub>2</sub> level is 417 ppm [85], which has increased by nearly 50% compared to the pre-industrial level. The atmospheric CO<sub>2</sub> concentrations will continue to rise until the end of this century unless a very stringent CO<sub>2</sub> emissions trajectory is satisfied (Representative Concentration Pathway 2.6) [86]. A large amount of atmospheric CO<sub>2</sub> traps and prevents heat from escaping the planet, driving global warming and subsequent climate change. As a natural carbon sink, the ocean has absorbed around 48% of anthropogenic CO<sub>2</sub> since the Industrial Revolution [87]. Given the elevated atmospheric CO<sub>2</sub> levels, more CO<sub>2</sub> has dissolved in the ocean. The dissolution of atmospheric CO<sub>2</sub> produces carbonic acid (H<sub>2</sub>CO<sub>3</sub>), which dissociates to form bicarbonate ions (HCO<sub>3</sub><sup>-</sup>) and hydrogen ions (H<sup>+</sup>). HCO<sub>3</sub><sup>-</sup> further dissociates into carbonate ions (CO<sub>3</sub><sup>2-</sup>) and H<sup>+</sup>. The rise in the concentration of H<sup>+</sup> in turn has acidified the ocean, resulting in OA. OA has altered the carbonate chemistry of the aquatic system. Excess H<sup>+</sup> released from the dissociation of dissolved CO<sub>2</sub> creates an imbalance in the carbonate equilibrium. The equilibrium is attained by the natural buffering capacity of the ocean. The free CO<sub>3</sub><sup>2-</sup> in the ocean binds with the excess H<sup>+</sup> to produce more HCO<sub>3</sub><sup>-</sup>. As a result, the dissolved CO<sub>2</sub> and HCO<sub>3</sub><sup>-</sup> concentrations increase while the CO<sub>3</sub><sup>2-</sup> levels decrease under OA. Since the decrease in CO<sub>3</sub><sup>2-</sup> levels leads to a lower saturation state of CaCO<sub>3</sub>, OA is particularly detrimental to marine-calcifying organisms such as molluscs, coccolithophores, and corals [88].

OA (increased pCO<sub>2</sub>/decreased pH) alters the carbon chemistry of the aquatic environment and acidifies the water. Microalgae have shown great adaptability towards different abiotic stress factors [89,90]. Therefore, it is believed that microalgae will respond and acclimate to OA by regulating their metabolic activities, which may in turn affect

their toxicity. However, the effects of OA on microalgal toxicity and the underlying mechanisms have not been well characterized. Apart from leading to shellfish poisoning in humans, several studies have indicated the bioaccumulation of algal toxins in predators of microalgae and the biomagnification of algal toxins through food webs, which cause disease or even death among marine organisms [91–95]. A recent study suggested that the bioavailability of STX would increase under global warming and ocean acidification [96]. Although the bioavailability of STX and other phycotoxins in high CO<sub>2</sub> conditions has not been fully examined, the possibility that more toxins can be accumulated along the food chain and harm the health of marine organisms and humans should not be neglected [96]. Predicting the toxicity of microalgae under OA is therefore important to evaluate the public health concerns and ecological impacts of intensified HABs in future high atmospheric CO<sub>2</sub> scenarios, which will provide insights for policymakers to improve the monitoring programs for HABs. Considering the above, this paper reviewed the effects of OA on the toxicity of microalgae, and the underlying mechanisms proposed.

### 3.1. Effects of OA on the Toxicity of Microalgae

No studies that investigated the effects of OA on the toxicity changes in microalgae that produce okadaic acid and azaspiracids could be found in the literature. Therefore, the scope of the review was limited to microalgae that synthesize STXs, DA, and PbTx. The experimental setups and significant findings of the reviewed studies are summarized in Table 1.

**Table 1.** Summary of reviewed studies on the effects of OA on toxigenic microalgae.

Algal Species (Strains)	OA Modeling Method	Experimental Parameters <sup>a</sup>		Significant Outcomes <sup>b</sup>	Reference
		Control	High pCO <sub>2</sub> Treatment		
<b>STXs-Producing Microalgae</b>					
<i>Alexandrium fundyense</i> (NBP8) isolated from Northport Bay	Laboratory culture CO <sub>2</sub> gas bubbling	Experiment No. 1 pH: 8.085 ± 0.009 A <sub>T</sub> : 1824 ± 87 μmol L <sup>-1</sup> Calculated pCO <sub>2</sub> : 41 ± 2 Pa DIC: 1600 ± 80 μmol L <sup>-1</sup> Length of experiment: 15 days	Experiment No. 1 pH: 7.629 ± 0.031 A <sub>T</sub> : 1678 ± 123 μmol L <sup>-1</sup> Calculated pCO <sub>2</sub> : 122 ± 6 Pa DIC: 1606 ± 116 μmol L <sup>-1</sup> Length of experiment: 15 days	Experiment No. 1 Growth rate increased *	[97]
		Experiment No. 2 pH: 8.068 ± 0.013 A <sub>T</sub> : 1858 ± 104 μmol L <sup>-1</sup> Calculated pCO <sub>2</sub> : 44 ± 4 Pa DIC: 1639 ± 100 μmol L <sup>-1</sup> Length of experiment: 27 days	Experiment No. 2 pH: 7.741 ± 0.007 A <sub>T</sub> : 1975 ± 128 μmol L <sup>-1</sup> Calculated pCO <sub>2</sub> : 110 ± 7 Pa DIC: 1868 ± 125 μmol L <sup>-1</sup> Length of experiment: 27 days	Experiment No. 2 Total cellular toxicity increased * GTX1/4 increased *	[97]

Table 1. Cont.

Algal Species (Strains)	OA Modeling Method	Experimental Parameters <sup>a</sup>		Significant Outcomes <sup>b</sup>	Reference
		Control	High pCO <sub>2</sub> Treatment		
<i>Alexandrium fundyense</i> (CCMP2304) isolated from the Bay of Fundy		Experiment No. 3 pH: 8.075 ± 0.057 A <sub>T</sub> : 1994 ± 355 μmol L <sup>-1</sup> Calculated pCO <sub>2</sub> : 46 ± 2 Pa DIC: 1790 ± 329 μmol L <sup>-1</sup> Length of experiment: 15 days	Experiment No. 3 pH: 7.545 ± 0.034 A <sub>T</sub> : 1966 ± 231 μmol L <sup>-1</sup> Calculated pCO <sub>2</sub> : 177 ± 9 Pa DIC: 1941 ± 243 μmol L <sup>-1</sup> Length of experiment: 15 days	Experiment No. 3 Growth rate increased *	[97]
		Experiment No. 4 pH: 8.096 ± 0.032 A <sub>T</sub> : 2122 ± 123 μmol L <sup>-1</sup> Calculated pCO <sub>2</sub> : 47 ± 2 Pa DIC: 1885 ± 102 μmol L <sup>-1</sup> Length of experiment: 12 days	Experiment No. 4 pH: 7.592 ± 0.022 A <sub>T</sub> : 1977 ± 240 μmol L <sup>-1</sup> Calculated pCO <sub>2</sub> : 162 ± 12 Pa DIC: 1977 ± 240 μmol L <sup>-1</sup> Length of experiment: 12 days	Experiment No. 4 Growth rate increased * Total cellular toxicity increased * GTX1/4 increased *	[97]
		Experiment No. 5 pH: 8.118 ± 0.008 A <sub>T</sub> : 2167 ± 53 μmol L <sup>-1</sup> Calculated pCO <sub>2</sub> : 45 ± 1 Pa DIC: 1912 ± 44 μmol L <sup>-1</sup> Length of experiment: 24 days	Experiment No. 5 pH: 7.873 ± 0.033 A <sub>T</sub> : 2186 ± 91 μmol L <sup>-1</sup> Calculated pCO <sub>2</sub> : 87 ± 4 Pa DIC: 2033 ± 71 μmol L <sup>-1</sup> Length of experiment: 24 days	Experiment No. 5 Growth rate: increased *	[97]
		Experiment No. 6 pH: 8.041 ± 0.012 A <sub>T</sub> : 1729 ± 56 μmol L <sup>-1</sup> Calculated pCO <sub>2</sub> : 44 ± 1 Pa DIC: 1539 ± 49 μmol L <sup>-1</sup> Length of experiment: 12 days	Experiment No. 6 pH: 7.547 ± 0.028 A <sub>T</sub> : 1889 ± 90 μmol L <sup>-1</sup> Calculated pCO <sub>2</sub> : 169 ± 4 Pa DIC: 1845 ± 84 μmol L <sup>-1</sup> Length of experiment: 12 days	Experiment No. 6 Growth rate increased *	[97]
		Experiment No. 7 pH: 8.086 ± 0.048 A <sub>T</sub> : 2121 ± 213 μmol L <sup>-1</sup> Calculated pCO <sub>2</sub> : 48 ± 3 Pa DIC: 1888 ± 183 μmol L <sup>-1</sup> Length of experiment: 12 days	Experiment No. 7 pH: 7.556 ± 0.038 A <sub>T</sub> : 2184 ± 167 μmol L <sup>-1</sup> Calculated pCO <sub>2</sub> : 191 ± 4 Pa DIC: 2138 ± 157 μmol L <sup>-1</sup> Length of experiment: 12 days	Experiment No. 7 Growth rate increased *	[97]

Table 1. Cont.

Algal Species (Strains)	OA Modeling Method	Experimental Parameters <sup>a</sup>		Significant Outcomes <sup>b</sup>	Reference
		Control	High pCO <sub>2</sub> Treatment		
<i>Alexandrium minutum</i> (AM-1) isolated from the South China Sea	Laboratory culture CO <sub>2</sub> gas bubbling	400 ppm CO <sub>2</sub> treatment Length of experiment: 37 days	800 ppm CO <sub>2</sub> treatment Length of experiment: 37 days	400 vs. 800 ppm CO <sub>2</sub> Total cellular toxicity increased **	[98]
		400 ppm CO <sub>2</sub> treatment Length of experiment: 37 days	1200 ppm CO <sub>2</sub> treatment Length of experiment: 37 days	400 vs. 1200 ppm CO <sub>2</sub> Total cellular toxicity increased **	[98]
<i>Alexandrium catenella</i> (A-11c) isolated from Jalama Beach	Laboratory culture CO <sub>2</sub> gas bubbling	380 µatm CO <sub>2</sub> treatment pH: 8.169 Calculated pCO <sub>2</sub> : 285 µatm DIC: 1957 µmol L <sup>-1</sup> Length of experiment: 7 days	750 µatm CO <sub>2</sub> treatment pH: 7.925 Calculated pCO <sub>2</sub> : 571 µatm DIC: 2103 µmol L <sup>-1</sup> Length of experiment: 7 days	380 vs. 750 µatm CO <sub>2</sub> Growth rate increased *** Total cellular toxicity increased ***	[99]
<i>Alexandrium ostenfeldii</i> (AON13) isolated from Ouwerkerkse Kreek		400 µatm CO <sub>2</sub> treatment pH: 8.23 ± 0.02 Calculated pCO <sub>2</sub> : 213 ± 11 µatm DIC: 1188 ± 41 µmol L <sup>-1</sup> Length of experiment: 14 days	1000 µatm CO <sub>2</sub> treatment pH: 7.82 ± 0.01 Calculated pCO <sub>2</sub> : 527 ± 30 µatm DIC: 1168 ± 56 µmol L <sup>-1</sup> Length of experiment: 14 days	400 vs. 1000 µatm CO <sub>2</sub> STX increased *	[100]
<i>Alexandrium ostenfeldii</i> (AON15) isolated from Ouwerkerkse Kreek	Laboratory culture CO <sub>2</sub> gas bubbling prior to cell inoculation <sup>c</sup>	400 µatm CO <sub>2</sub> treatment pH: 8.07 ± 0.07 Calculated pCO <sub>2</sub> : 357 ± 36 µatm DIC: 1120 ± 21 µmol L <sup>-1</sup> Length of experiment: 14 days	1000 µatm CO <sub>2</sub> treatment pH: 7.75 ± 0.08 Calculated pCO <sub>2</sub> : 676 ± 55 µatm DIC: 1117 ± 10 µmol L <sup>-1</sup> Length of experiment: 14 days	400 vs. 1000 µatm CO <sub>2</sub> Growth rate increased ** Total cellular toxicity decreased *** GTX increased *	[100]
<i>Alexandrium ostenfeldii</i> (AON5.26) isolated from Ouwerkerkse Kreek		400 µatm CO <sub>2</sub> treatment pH: 8.17 ± 0.05 Calculated pCO <sub>2</sub> : 286 ± 13 µatm DIC: 1085 ± 15 µmol L <sup>-1</sup> Length of experiment: 14 days	1000 µatm CO <sub>2</sub> treatment pH: 7.86 ± 0.03 Calculated pCO <sub>2</sub> : 479 ± 18 µatm DIC: 1126 ± 2 µmol L <sup>-1</sup> Length of experiment: 14 days	Growth rate increased *** GTX increased *** STX and C1/2 decreased ***	[100]

Table 1. Cont.

Algal Species (Strains)	OA Modeling Method	Experimental Parameters <sup>a</sup>		Significant Outcomes <sup>b</sup>	Reference
		Control	High pCO <sub>2</sub> Treatment		
<i>Alexandrium tamarense</i> (Alex5)	Laboratory culture CO <sub>2</sub> gas bubbling	380 µatm CO <sub>2</sub> treatment pH: 8.27 ± 0.07 A <sub>T</sub> : 2439 ± 1 µmol L <sup>-1</sup> Calculated pCO <sub>2</sub> : 315 ± 57 µatm DIC: 2117 ± 41 µmol L <sup>-1</sup> Length of experiment: 8 days	800 µatm CO <sub>2</sub> treatment pH: 7.97 ± 0.10 A <sub>T</sub> : 2434 ± 2 µmol L <sup>-1</sup> Calculated pCO <sub>2</sub> : 706 ± 154 µatm DIC: 2245 ± 37 µmol L <sup>-1</sup> Length of experiment: 8 days	380 vs. 800 µatm CO <sub>2</sub> Total cellular toxicity decreased * Non-sulfated STX analogues decreased * Di-sulfated STX analogues increased *	[101]
		380 µatm CO <sub>2</sub> treatment pH: 8.27 ± 0.07 A <sub>T</sub> : 2439 ± 1 µmol L <sup>-1</sup> Calculated pCO <sub>2</sub> : 315 ± 57 µatm DIC: 2117 ± 41 µmol L <sup>-1</sup> Length of experiment: 8 days	1200 µatm CO <sub>2</sub> treatment pH: 7.83 ± 0.12 A <sub>T</sub> : 2418 ± 1 µmol L <sup>-1</sup> Calculated pCO <sub>2</sub> : 995 ± 248 µatm DIC: 2283 ± 34 µmol L <sup>-1</sup> Length of experiment: 8 days	380 vs. 1200 µatm CO <sub>2</sub> Total cellular toxicity decreased * Non-sulfated STX analogues decreased * Mono-sulfated STX analogues increased * Di-sulfated STX analogues increased *	[101]
<i>Alexandrium tamarense</i> (Alex2)	Laboratory culture CO <sub>2</sub> gas bubbling	380 µatm CO <sub>2</sub> treatment pH: 8.27 ± 0.02 A <sub>T</sub> : 2384 ± 4 µmol L <sup>-1</sup> Calculated pCO <sub>2</sub> : 305 ± 20 µatm DIC: 2111 ± 14 µmol L <sup>-1</sup> Length of experiment: 8 days	800 µatm CO <sub>2</sub> treatment pH: 7.90 ± 0.03 A <sub>T</sub> : 2390 ± 6 µmol L <sup>-1</sup> Calculated pCO <sub>2</sub> : 810 ± 60 µatm DIC: 2229 ± 33 µmol L <sup>-1</sup> Length of experiment: 8 days	380 vs. 800 µatm CO <sub>2</sub> No significant changes in growth rate, total cellular toxicity, and toxin profile	[101]
		380 µatm CO <sub>2</sub> treatment pH: 8.27 ± 0.02 A <sub>T</sub> : 2384 ± 4 µmol L <sup>-1</sup> Calculated pCO <sub>2</sub> : 305 ± 20 µatm DIC: 2111 ± 14 µmol L <sup>-1</sup> Length of experiment: 8 days	1200 µatm CO <sub>2</sub> treatment pH: 7.75 ± 0.04 A <sub>T</sub> : 2386 ± 9 µmol L <sup>-1</sup> Calculated pCO <sub>2</sub> : 1167 ± 112 µatm DIC: 2279 ± 14 µmol L <sup>-1</sup> Length of experiment: 8 days	380 vs. 1200 µatm CO <sub>2</sub> No significant changes in growth rate, total cellular toxicity, and toxin profile	[101]

Table 1. Cont.

Algal Species (Strains)	OA Modeling Method	Experimental Parameters <sup>a</sup>		Significant Outcomes <sup>b</sup>	Reference
		Control	High pCO <sub>2</sub> Treatment		
<b>DA-producing microalgae</b>					
<i>Pseudo-nitzschia multiseri</i> (CCMP2708) isolated from Eastern Canada	Laboratory culture CO <sub>2</sub> gas bubbling	22 Pa CO <sub>2</sub> treatment pH: 8.40 ± 0.03 Calculated pCO <sub>2</sub> : 22 ± 2 Pa DIC: 1970 ± 4 μmol L <sup>-1</sup> Length of experiment: around 4 to 6 weeks	41 Pa CO <sub>2</sub> treatment pH: 8.19 ± 0.02 Calculated pCO <sub>2</sub> : 40 ± 3 Pa DIC: 2066 ± 11 μmol L <sup>-1</sup> Length of experiment: around 4 to 6 weeks	22 vs. 41 Pa CO <sub>2</sub> Growth rate increased *** Carbon fixation rate increased **	[102]
		22 Pa CO <sub>2</sub> treatment pH: 8.40 ± 0.03 Calculated pCO <sub>2</sub> : 22 ± 2 Pa DIC: 1970 ± 4 μmol L <sup>-1</sup> Length of experiment: around 4 to 6 weeks	74 Pa CO <sub>2</sub> treatment pH: 7.96 ± 0.01 Calculated pCO <sub>2</sub> : 73 ± 1 Pa DIC: 2177 ± 6 μmol L <sup>-1</sup> Length of experiment: around 4 to 6 weeks	22 vs. 74 Pa CO <sub>2</sub> Growth rate increased *** Carbon fixation rate increased *** Cellular DA content increased ***	[102]
		41 Pa CO <sub>2</sub> treatment pH: 8.19 ± 0.02 Calculated pCO <sub>2</sub> : 40 ± 3 Pa DIC: 2066 ± 11 μmol L <sup>-1</sup> Length of experiment: around 4 to 6 weeks	74 Pa CO <sub>2</sub> treatment pH: 7.96 ± 0.01 Calculated pCO <sub>2</sub> : 73 ± 1 Pa DIC: 2177 ± 6 μmol L <sup>-1</sup> Length of experiment: around 4 to 6 weeks	41 vs. 74 Pa CO <sub>2</sub> Growth rate increased *** Cellular DA content increased **	[102]
<i>Pseudo-nitzschia fraudulenta</i> isolated from Ventura County	Laboratory culture CO <sub>2</sub> gas bubbling	200 ppm CO <sub>2</sub> treatment pH: 8.43 Calculated pCO <sub>2</sub> : 198 ppm DIC: 1965 μmol L <sup>-1</sup>	360 ppm CO <sub>2</sub> treatment pH: 8.23 Calculated pCO <sub>2</sub> : 357 ppm DIC: 2107 μmol L <sup>-1</sup>	200 vs. 360 ppm CO <sub>2</sub> Growth rate increased *** Carbon fixation rate increased	[103]
		200 ppm CO <sub>2</sub> treatment pH: 8.43 Calculated pCO <sub>2</sub> : 198 ppm DIC: 1965 μmol L <sup>-1</sup>	765 ppm CO <sub>2</sub> treatment pH: 7.95 Calculated pCO <sub>2</sub> : 764 ppm DIC: 2249 μmol L <sup>-1</sup>	200 vs. 765 ppm CO <sub>2</sub> Growth rate increased *** Carbon fixation rate increased	[103]

Table 1. Cont.

Algal Species (Strains)	OA Modeling Method	Experimental Parameters <sup>a</sup>		Significant Outcomes <sup>b</sup>	Reference
		Control	High pCO <sub>2</sub> Treatment		
<i>Pseudo-nitzschia australis</i> (HAB 200) isolated from northern Monterey Bay	Laboratory culture CO <sub>2</sub> gas bubbling	pH 8.1 treatment Length of experiment: 7 days Exponential growth phase pH: 8.14 ± 0.01 A <sub>T</sub> : 2232 ± 9 μmol L <sup>-1</sup> Calculated pCO <sub>2</sub> : 406 ± 8 μatm DIC: 2032 ± 11 μmol L <sup>-1</sup> Stationary growth phase pH: 8.14 ± 0.01 A <sub>T</sub> : 2239 ± 25 μmol L <sup>-1</sup> Calculated pCO <sub>2</sub> : 410 ± 2 μatm DIC: 2052 ± 21 μmol L <sup>-1</sup>	pH 8.0 treatment Length of experiment: 8 days Exponential growth phase pH: 8.03 ± 0.01 A <sub>T</sub> : 2248 ± 25 μmol L <sup>-1</sup> Calculated pCO <sub>2</sub> : 550 ± 8 μatm DIC: 2093 ± 21 μmol L <sup>-1</sup> Stationary growth phase pH: 8.04 ± 0.01 A <sub>T</sub> : 2254 ± 14 μmol L <sup>-1</sup> Calculated pCO <sub>2</sub> : 537 ± 19 μatm DIC: 2107 ± 17 μmol L <sup>-1</sup>	pH 8.1 vs. pH 8.0 No significant response	[104]
		pH 8.1 treatment Length of experiment: 7 days Exponential growth phase pH: 8.14 ± 0.01 A <sub>T</sub> : 2232 ± 9 μmol L <sup>-1</sup> Calculated pCO <sub>2</sub> : 406 ± 8 μatm DIC: 2032 ± 11 μmol L <sup>-1</sup> Stationary growth phase pH: 8.14 ± 0.01 A <sub>T</sub> : 2239 ± 25 μmol L <sup>-1</sup> Calculated pCO <sub>2</sub> : 410 ± 2 μatm DIC: 2052 ± 21 μmol L <sup>-1</sup>	pH 7.9 treatment Length of experiment: 8 days Exponential growth phase pH: 7.93 ± 0.02 A <sub>T</sub> : 2255 ± 20 μmol L <sup>-1</sup> Calculated pCO <sub>2</sub> : 719 ± 34 μatm DIC: 2136 ± 25 μmol L <sup>-1</sup> Stationary growth phase pH: 7.93 ± 0.02 A <sub>T</sub> : 2279 ± 14 μmol L <sup>-1</sup> Calculated pCO <sub>2</sub> : 732 ± 28 μatm DIC: 2175 ± 13 μmol L <sup>-1</sup>	pH 8.1 vs. pH 7.9 Maximum carbon fixation rate increased **	[104]

Table 1. Cont.

Algal Species (Strains)	OA Modeling Method	Experimental Parameters <sup>a</sup>		Significant Outcomes <sup>b</sup>	Reference
		Control	High pCO <sub>2</sub> Treatment		
		pH 8.0 treatment Length of experiment: 8 days Exponential growth phase pH: 8.03 ± 0.01 A <sub>T</sub> : 2248 ± 25 μmol L <sup>-1</sup> Calculated pCO <sub>2</sub> : 550 ± 8 μatm DIC: 2093 ± 21 μmol L <sup>-1</sup> Stationary growth phase pH: 8.04 ± 0.01 A <sub>T</sub> : 2254 ± 14 μmol L <sup>-1</sup> Calculated pCO <sub>2</sub> : 537 ± 19 μatm DIC: 2107 ± 17 μmol L <sup>-1</sup>	pH 7.9 treatment Length of experiment: 8 days Exponential growth phase pH: 7.93 ± 0.02 A <sub>T</sub> : 2255 ± 20 μmol L <sup>-1</sup> Calculated pCO <sub>2</sub> : 719 ± 34 μatm DIC: 2136 ± 25 μmol L <sup>-1</sup> Stationary growth phase pH: 7.93 ± 0.02 A <sub>T</sub> : 2279 ± 14 μmol L <sup>-1</sup> Calculated pCO <sub>2</sub> : 732 ± 28 μatm DIC: 2175 ± 13 μmol L <sup>-1</sup>	pH 8.0 vs. pH 7.9 Maximum carbon fixation rate increased *	[104]
		pH 8.1 treatment Length of experiment: 7 days Exponential growth phase pH: 8.14 ± 0.01 A <sub>T</sub> : 2232 ± 9 μmol L <sup>-1</sup> Calculated pCO <sub>2</sub> : 406 ± 8 μatm DIC: 2032 ± 11 μmol L <sup>-1</sup> Stationary growth phase pH: 8.14 ± 0.01 A <sub>T</sub> : 2239 ± 25 μmol L <sup>-1</sup> Calculated pCO <sub>2</sub> : 410 ± 2 μatm DIC: 2052 ± 21 μmol L <sup>-1</sup>	pH 7.8 treatment Length of experiment: 9 days Exponential growth phase pH: 7.81 ± 0.03 A <sub>T</sub> : 2292 ± 3 μmol L <sup>-1</sup> Calculated pCO <sub>2</sub> : 980 ± 64 μatm DIC: 2213 ± 11 μmol L <sup>-1</sup> Stationary growth phase pH: 7.84 ± 0.01 A <sub>T</sub> : 2348 ± 17 μmol L <sup>-1</sup> Calculated pCO <sub>2</sub> : 929 ± 12 μatm DIC: 2271 ± 16 μmol L <sup>-1</sup>	pH 8.1 vs. pH 7.8 Growth rate decreased **** Maximum carbon fixation rate increased *	[104]

Table 1. Cont.

Algal Species (Strains)	OA Modeling Method	Experimental Parameters <sup>a</sup>		Significant Outcomes <sup>b</sup>	Reference
		Control	High pCO <sub>2</sub> Treatment		
		pH 8.0 treatment Length of experiment: 8 days Exponential growth phase pH: 8.03 ± 0.01 A <sub>T</sub> : 2248 ± 25 μmol L <sup>-1</sup> Calculated pCO <sub>2</sub> : 550 ± 8 μatm DIC: 2093 ± 21 μmol L <sup>-1</sup> Stationary growth phase pH: 8.04 ± 0.01 A <sub>T</sub> : 2254 ± 14 μmol L <sup>-1</sup> Calculated pCO <sub>2</sub> : 537 ± 19 μatm DIC: 2107 ± 17 μmol L <sup>-1</sup>	pH 7.8 treatment Length of experiment: 9 days Exponential growth phase pH: 7.81 ± 0.03 A <sub>T</sub> : 2292 ± 3 μmol L <sup>-1</sup> Calculated pCO <sub>2</sub> : 980 ± 64 μatm DIC: 2213 ± 11 μmol L <sup>-1</sup> Stationary growth phase pH: 7.84 ± 0.01 A <sub>T</sub> : 2348 ± 17 μmol L <sup>-1</sup> Calculated pCO <sub>2</sub> : 929 ± 12 μatm DIC: 2271 ± 16 μmol L <sup>-1</sup>	pH 8.0 vs. pH 7.8 Growth rate decreased **** Maximum carbon fixation rate increased *	[104]
		pH 7.9 treatment Length of experiment: 8 days Exponential growth phase pH: 7.93 ± 0.02 A <sub>T</sub> : 2255 ± 20 μmol L <sup>-1</sup> Calculated pCO <sub>2</sub> : 719 ± 34 μatm DIC: 2136 ± 25 μmol L <sup>-1</sup> Stationary growth phase pH: 7.93 ± 0.02 A <sub>T</sub> : 2279 ± 14 μmol L <sup>-1</sup> Calculated pCO <sub>2</sub> : 732 ± 28 μatm DIC: 2175 ± 13 μmol L <sup>-1</sup>	pH 7.8 treatment Length of experiment: 9 days Exponential growth phase pH: 7.81 ± 0.03 A <sub>T</sub> : 2292 ± 3 μmol L <sup>-1</sup> Calculated pCO <sub>2</sub> : 980 ± 64 μatm DIC: 2213 ± 11 μmol L <sup>-1</sup> Stationary growth phase pH: 7.84 ± 0.01 A <sub>T</sub> : 2348 ± 17 μmol L <sup>-1</sup> Calculated pCO <sub>2</sub> : 929 ± 12 μatm DIC: 2271 ± 16 μmol L <sup>-1</sup>	pH 7.9 vs. pH 7.8 Growth rate Decreased ****	[104]
<i>Pseudo-nitzschia</i> spp. in Gullmar Fjord	Mesocosm, addition of CO <sub>2</sub> -saturated seawater	380 μatm CO <sub>2</sub> treatment Length of experiment: 111 days	1000 μatm CO <sub>2</sub> treatment Calculated pCO <sub>2</sub> : 760 ± 175 μatm Length of experiment: 111 days	380 vs. 1000 μatm CO <sub>2</sub> Cellular DA content increased *	[105]

Table 1. Cont.

Algal Species (Strains)	OA Modeling Method	Experimental Parameters <sup>a</sup>		Significant Outcomes <sup>b</sup>	Reference
		Control	High pCO <sub>2</sub> Treatment		
<b>PbTx-producing microalgae</b>					
<i>Karenia brevis</i> (CCFWC-126) isolated from the Gulf of Mexico	Laboratory culture CO <sub>2</sub> gas bubbling	150 µatm CO <sub>2</sub> treatment Before inoculation pH: 8.51 ± 0.04 A <sub>T</sub> : 2320 ± 3 µmol L <sup>-1</sup> Calculated pCO <sub>2</sub> : 118.9 ± 0.1 µatm DIC: 1679 ± 2 µmol L <sup>-1</sup> Mid exponential phase pH: 8.63 ± 0.05 A <sub>T</sub> : 2428 ± 64 µmol L <sup>-1</sup> Calculated pCO <sub>2</sub> : 102.9 ± 16.8 µatm DIC: 1714 ± 4 µmol L <sup>-1</sup>	400 µatm CO <sub>2</sub> treatment Before inoculation pH: 8.12 ± 0.02 A <sub>T</sub> : 2348 ± 18 µmol L <sup>-1</sup> Calculated pCO <sub>2</sub> : 446.6 ± 31.0 µatm DIC: 2008 µmol L <sup>-1</sup> Mid exponential phase pH: 8.22 ± 0.03 A <sub>T</sub> : 2376 ± 14 µmol L <sup>-1</sup> Calculated pCO <sub>2</sub> : 355.6 ± 30.4 µatm DIC: 1982 ± 26 µmol L <sup>-1</sup>	150 vs. 400 µatm CO <sub>2</sub> No significant response	[106]
		150 µatm CO <sub>2</sub> treatment Before inoculation pH: 8.51 ± 0.04 A <sub>T</sub> : 2320 ± 3 µmol L <sup>-1</sup> Calculated pCO <sub>2</sub> : 118.9 ± 0.1 µatm DIC: 1679 ± 2 µmol L <sup>-1</sup> Mid exponential phase pH: 8.63 ± 0.05 A <sub>T</sub> : 2428 ± 64 µmol L <sup>-1</sup> Calculated pCO <sub>2</sub> : 102.9 ± 16.8 µatm DIC: 1714 ± 4 µmol L <sup>-1</sup>	780 µatm CO <sub>2</sub> treatment Before inoculation pH: 7.89 ± 0.01 A <sub>T</sub> : 2309 ± 1 µmol L <sup>-1</sup> Calculated pCO <sub>2</sub> : 812.7 ± 0.5 µatm DIC: 2089 ± 1 µmol L <sup>-1</sup> Mid exponential phase pH: 7.95 ± 0.04 A <sub>T</sub> : 2342 ± 19 µmol L <sup>-1</sup> Calculated pCO <sub>2</sub> : 753.4 ± 78.8 µatm DIC: 2103 ± 4 µmol L <sup>-1</sup>	150 vs. 780 µatm CO <sub>2</sub> No significant response	[106]

Table 1. Cont.

Algal Species (Strains)	OA Modeling Method	Experimental Parameters <sup>a</sup>		Significant Outcomes <sup>b</sup>	Reference
		Control	High pCO <sub>2</sub> Treatment		
		400 µatm CO <sub>2</sub> treatment Before inoculation pH: 8.12 ± 0.02 A <sub>T</sub> : 2348 ± 18 µmol L <sup>-1</sup> Calculated pCO <sub>2</sub> : 446.6 ± 31.0 µatm DIC: 2008 µmol L <sup>-1</sup> Mid exponential phase pH: 8.22 ± 0.03 A <sub>T</sub> : 2376 ± 14 µmol L <sup>-1</sup> Calculated pCO <sub>2</sub> : 355.6 ± 30.4 µatm DIC: 1982 ± 26 µmol L <sup>-1</sup>	780 µatm CO <sub>2</sub> treatment Before inoculation pH: 7.89 ± 0.01 A <sub>T</sub> : 2309 ± 1 µmol L <sup>-1</sup> Calculated pCO <sub>2</sub> : 812.7 ± 0.5 µatm DIC: 2089 ± 1 µmol L <sup>-1</sup> Mid exponential phase pH: 7.95 ± 0.04 A <sub>T</sub> : 2342 ± 19 µmol L <sup>-1</sup> Calculated pCO <sub>2</sub> : 753.4 ± 78.8 µatm DIC: 2103 ± 4 µmol L <sup>-1</sup>	400 vs. 780 µatm CO <sub>2</sub> No significant response	[106]
<i>Karenia brevis</i> (Wilson) isolated from John's Pass	Laboratory culture CO <sub>2</sub> gas bubbling prior to cell inoculation <sup>2</sup>	250 ppm CO <sub>2</sub> treatment Length of experiment: 9 days Before inoculation Calculated pCO <sub>2</sub> : 241.2 µatm DIC: 1727.3 ± 33 µmol L <sup>-1</sup> At the beginning of the experiment A <sub>T</sub> : 2082.8 ± 34.3 µmol L <sup>-1</sup> Calculated pCO <sub>2</sub> : 134.2 µatm At the end of the experiment A <sub>T</sub> : 2198.6 ± 62.0 µmol L <sup>-1</sup> Calculated pCO <sub>2</sub> : 80.5 µatm DIC: 1562.6 ± 14.5 µmol L <sup>-1</sup>	350 ppm CO <sub>2</sub> treatment Length of experiment: 9 days Before inoculation Calculated pCO <sub>2</sub> : 318.4 µatm DIC: 1733.9 ± 163.7 µmol L <sup>-1</sup> At the beginning of the experiment A <sub>T</sub> : 2021.3 ± 33.6 µmol L <sup>-1</sup> Calculated pCO <sub>2</sub> : 115.6 µatm At the end of the experiment A <sub>T</sub> : 2250.5 ± 0.6 µmol L <sup>-1</sup> Calculated pCO <sub>2</sub> : 55.1 µatm DIC: 1509.9 ± 259.7 µmol L <sup>-1</sup>	No significant response	[107]

Table 1. Cont.

Algal Species (Strains)	OA Modeling Method	Experimental Parameters <sup>a</sup>		Significant Outcomes <sup>b</sup>	Reference
		Control	High pCO <sub>2</sub> Treatment		
		250 ppm CO <sub>2</sub> treatment Length of experiment: 9 days Before inoculation Calculated pCO <sub>2</sub> : 241.2 μatm DIC: 1727.3 ± 33 μmol L <sup>-1</sup> At the beginning of the experiment A <sub>T</sub> : 2082.8 ± 34.3 μmol L Calculated pCO <sub>2</sub> : 134.2 μatm At the end of the experiment A <sub>T</sub> : 2198.6 ± 62.0 μmol L <sup>-1</sup> Calculated pCO <sub>2</sub> : 80.5 μatm DIC: 1562.6 ± 14.5 μmol L <sup>-1</sup>	1000 ppm CO <sub>2</sub> treatment Length of experiment: 9 days Before inoculation Calculated pCO <sub>2</sub> : 1131.9 μatm DIC: 1986 ± 17.2 μmol L <sup>-1</sup> At the beginning of the experiment A <sub>T</sub> : 2076.6 ± 6 μmol L <sup>-1</sup> Calculated pCO <sub>2</sub> : 438.9 μatm At the end of the experiment A <sub>T</sub> : 2224.7 ± 10.7 μmol L <sup>-1</sup> Calculated pCO <sub>2</sub> : 166.1 μatm DIC: 1750.8 ± 21.1 μmol L <sup>-1</sup>	250 vs. 1000 ppm CO <sub>2</sub> Growth rate increased ***	[107]
		350 ppm CO <sub>2</sub> treatment Length of experiment: 9 days Before inoculation Calculated pCO <sub>2</sub> : 318.4 μatm DIC: 1733.9 ± 163.7 μmol L <sup>-1</sup> At the beginning of the experiment A <sub>T</sub> : 2021.3 ± 33.6 μmol L <sup>-1</sup> Calculated pCO <sub>2</sub> : 115.6 μatm At the end of the experiment A <sub>T</sub> : 2250.5 ± 0.6 μmol L <sup>-1</sup> Calculated pCO <sub>2</sub> : 55.1 μatm DIC: 1509.9 ± 259.7 μmol L <sup>-1</sup>	1000 ppm CO <sub>2</sub> treatment Length of experiment: 9 days Before inoculation Calculated pCO <sub>2</sub> : 1131.9 μatm DIC: 1986 ± 17.2 μmol L <sup>-1</sup> At the beginning of the experiment A <sub>T</sub> : 2076.6 ± 6 μmol L <sup>-1</sup> Calculated pCO <sub>2</sub> : 438.9 μatm At the end of the experiment A <sub>T</sub> : 2224.7 ± 10.7 μmol L <sup>-1</sup> Calculated pCO <sub>2</sub> : 166.1 μatm DIC: 1750.8 ± 21.1 μmol L <sup>-1</sup>	350 vs. 1000 ppm CO <sub>2</sub> Growth rate increased ***	[107]

Table 1. Cont.

Algal Species (Strains)	OA Modeling Method	Experimental Parameters <sup>a</sup>		Significant Outcomes <sup>b</sup>	Reference
		Control	High pCO <sub>2</sub> Treatment		
<i>Karenia brevis</i> (SP1) isolated from South Padre Island		300 ppm CO <sub>2</sub> treatment	1000 ppm CO <sub>2</sub> treatment	300 vs. 1000 ppm CO <sub>2</sub> Growth rate increased	[107]
		Length of experiment: 9 days	Length of experiment: 9 days		
		Before inoculation	Before inoculation		
		Calculated pCO <sub>2</sub> : 299 ± 157.8 µatm	Calculated pCO <sub>2</sub> : 1084 ± 14.1 µatm		
		At the beginning of the experiment	At the beginning of the experiment		
		Calculated pCO <sub>2</sub> : 211.8 ± 32 µatm	Calculated pCO <sub>2</sub> : 398.6 ± 3.4 µatm		
At the end of the experiment	At the end of the experiment				
		Calculated pCO <sub>2</sub> : 99 ± 32.7 µatm	Calculated pCO <sub>2</sub> : 219 ± 11.1 µatm		

<sup>a</sup> A<sub>T</sub>: total alkalinity, DIC: dissolved inorganic carbon. Length of experiment does not include pre-acclimation period of culture. <sup>b</sup> Significant outcomes refer to the significant differences in the growth rates, carbon fixation rates, and/or the toxicity observed between the corresponding control and high CO<sub>2</sub> treatment. \* =  $p \leq 0.05$ , \*\* =  $p \leq 0.01$ , \*\*\* =  $p \leq 0.001$ , \*\*\*\* =  $p \leq 0.0001$ . <sup>c</sup> Seawater was manipulated once by CO<sub>2</sub> gas bubbling before cell inoculation.

### 3.1.1. STXs-Producing Microalgae

Dinoflagellates from the genus *Alexandrium* are the most studied STX producers. However, there is not yet any solid conclusion drawn for the toxicity change in *Alexandrium* at elevated pCO<sub>2</sub>. Increases in cellular toxin levels were detected in *A. catenella*, *A. minutum*, and *A. fundyense* after high CO<sub>2</sub> treatment [97–99]. It is believed that elevated pCO<sub>2</sub> will permit microalgae to perform photosynthesis when more substrates are available for their unsaturated carbon-fixing enzyme ribulose-1,5-bisphosphate carboxylase-oxygenase (Rubisco) [108]. Dinoflagellates may be particularly sensitive to elevated pCO<sub>2</sub> as they possess type II Rubisco, which has a higher affinity with O<sub>2</sub>, a competitive inhibitor of CO<sub>2</sub> [109]. Since carbon is essential for the synthesis of biomolecules, including phycotoxins, increased production of fixed carbon at elevated pCO<sub>2</sub> may thus contribute to the higher toxicity of microalgae [99]. However, the carbon fixation rates of *A. catenella*, *A. minutum*, and *A. fundyense* after high CO<sub>2</sub> treatment were not measured to support this hypothesis.

Another plausible explanation for the enhanced production of STXs is the increased availability of STX precursors [98]. To initiate the synthesis of STX, arginine (Arg), methionine (Met), and acetate are required [110]. In the study performed by Lian, Li, He, Chen, and Yu [98], the concentrations of Arg and Met were quantified in *A. minutum* at elevated pCO<sub>2</sub>. It was found that the content of Arg and Met increased at the beginning of the experiment and then decreased gradually. The increase in the Arg level was related to the enhanced activity of argininosuccinate synthase, an enzyme responsible for a rate-limiting step in Arg synthesis. However, the mechanisms behind the rise in the Met level remained undetermined. Since the STX content increased after the decline in Arg and Met levels with a slight delay, it was suggested that elevated pCO<sub>2</sub> had indirectly promoted STX production by increasing Arg and Met supplies.

On the other hand, significant decreases in STX content were detected in both *A. tamarensense* and *A. ostenfeldii* at elevated pCO<sub>2</sub>, resulting in lower toxicity [100,101]. Van de Waal, Eberlein, John, Wohlrab, and Rost [101] isolated the RNA of *A. tamarensense* cultured at different pCO<sub>2</sub> (180, 380, 800, 1200 ppm) to perform microarray-based gene expression analysis. When comparing the 800 ppm group to the 380 ppm group (control), 1238 differentially expressed genes (DEGs) were found. Genes associated with amino acid

transport and metabolism were downregulated, implying that fewer Arg and Met molecules were synthesized and available for STX biosynthesis at elevated pCO<sub>2</sub>.

The differences in the toxicity of *Alexandrium* species may be caused by genetic variations between species. The gene expression patterns of the toxic *A. fundyense* and *A. tamarensense* strains revealed by Taroncher-Oldenburg and Anderson [111] indicated the high interspecific variations between them. In parallel with this previous finding, *A. fundyense* and *A. tamarensense* responded differently under OA. While *A. fundyense* promoted STX production at elevated pCO<sub>2</sub> [97], *A. tamarensense* inhibited STX production by reducing the synthesis of STX precursors [101]. The *Alexandrium* species are likely to regulate their metabolism differently under OA due to the interspecific variations in genetic expression, thus contributing to the toxicity differences.

Regarding the STX composition of *Alexandrium*, increased GTX1/4 is a common change observed in *A. catenella* and *A. tamarensense*, although the toxin profiles of *Alexandrium* are highly varied [99,101,112]. According to the gene expression profile of *A. tamarensense*, sulfur metabolism was differentially regulated under high CO<sub>2</sub> treatment [101]. The significant upregulation of a putative *sxtN* homologue encoding a sulfotransferase involved in synthesizing sulfated STXs was found [113–116]. In contrast, genes encoding sulfatases that are responsible for the hydrolysis of sulfate esters were downregulated. Together, they might promote the transformation of non-sulfated STXs to sulfated STXs while inhibiting the transformation of sulfated STXs to non-sulfated STXs. Moreover, the downregulation of genes encoding sulfite reductase was reported. Inhibition of assimilated sulfur into amino acids might result in more sulfur being allocated for synthesizing sulfated STXs [117,118]. In parallel with these, lower non-sulfated STX content but higher sulfated GTX1/4 and C1/2 content of *A. tamarensense* at elevated pCO<sub>2</sub> were observed. Nevertheless, increases in both non-sulfated and sulfated STX levels were exhibited in *A. catenella* after high CO<sub>2</sub> treatment [99], suggesting that the toxin composition could be altered by different metabolic pathways besides sulfur metabolism.

### 3.1.2. DA-Producing Microalgae

The diatom *Pseudo-nitzschia* has been extensively studied compared to other DA producers. Generally, both laboratory and mesocosm studies revealed increased cellular DA content of *Pseudo-nitzschia* at elevated pCO<sub>2</sub> [102–105]. In line with the assumption that excess fixed carbon may be shunted for toxin biosynthesis in microalgae under OA [99], an increased growth rate, carbon fixation rate, and cellular DA content were reported in *P. fraudulenta* at elevated pCO<sub>2</sub> [103]. Nonetheless, there were no consistent findings of *P. australis* [104]. The cellular DA content of *P. australis* was largely unchanged despite the increased carbon fixation rate at elevated pCO<sub>2</sub>.

For DA-producing *Pseudo-nitzschia*, environmental pH may also play a role in toxin biosynthesis by affecting cellular enzymatic activities, metal speciation, and the composition of symbiotic bacteria [119]. The intracellular pH of diatoms may be modified or maintained by regulating the metabolism under acidification [120]. Although research on the intracellular pH change of *Pseudo-nitzschia* at elevated pCO<sub>2</sub> is lacking, the effects of acidification on DA biosynthesis should not be neglected. Lundholm, Hansen, and Kotaki [119] proposed that there might be an optimal pH for DA biosynthesis; however, it remains to be determined as an increased cellular DA level was detected under both low and high pH conditions in *Pseudo-nitzschia* [102,103,119,121]. The DA biosynthetic pathway has been modeled recently based on the transcriptome sequencing of *P. multiseriata* [122]. The intracellular pH of *Pseudo-nitzschia* may be modified under acidification, which possibly affects the activities of putative DA biosynthetic (Dab) enzymes including terpene cyclase (*dabA*), hypothetical protein (*dabB*), alpha-ketoglutarate-dependent dioxygenase (*dabC*), and CYP450 (*dabD*), causing changes in cellular DA content.

The toxicity and availability of metals are likely to be affected by a decreased pH. For example, a rise in the concentrations of free copper (Cu<sup>2+</sup>) and dissolved iron (Fe<sup>3+</sup>) was expected at lower pH levels due to increased solubility [123]. While the Cu<sup>2+</sup> level is

generally closely related to its toxicity in phytoplankton [124],  $\text{Fe}^{3+}$  is one of the essential micronutrients for microalgal growth. Although the ecological and physiological roles of DA have not been well established, it was suggested that DA might be a trace metal chelator involved in iron acquisition and copper detoxification, given its similar structure to phytosiderophores [125]. Therefore, increases in  $\text{Cu}^{2+}$  and  $\text{Fe}^{3+}$  levels under an acidic environment may stimulate the DA production of *Pseudo-nitzschia*. However, both the cellular and dissolved DA content of *P. multiseriis* remained largely unchanged after exposure to different copper levels [126]. On the other hand, a positive relationship between the iron concentration and total DA content in *P. multiseriis* was indicated [127]. Thus, enhanced DA production at elevated  $\text{pCO}_2$  may be mainly contributed by the increased concentration of  $\text{Fe}^{3+}$  rather than  $\text{Cu}^{2+}$  under acidification.

Symbiotic bacteria are related to DA biosynthesis in *Pseudo-nitzschia*. Xenic cultures of *P. multiseriis* exhibited increased DA content when compared with axenic cultures [128]. While free-living bacteria were likely to be incapable of producing DA autonomously [129,130], it is difficult to obtain a conclusion for epiphytic bacteria due to the difficulties in isolating them from the diatoms. Research on the bacteria–phytoplankton interaction mechanisms for DA biosynthesis in *Pseudo-nitzschia* is lacking. However, it was proposed that the attached bacteria might exchange metabolites that are used for DA biosynthesis with *Pseudo-nitzschia* [130]. Since bacterial abundance and diversity were shown to be affected by a decreased environmental pH [131], symbiotic bacteria that promote DA biosynthesis may become more abundant at lower pH levels given the observation of increased cellular DA content in *Pseudo-nitzschia*.

### 3.1.3. PbTx-Producing Microalgae

Dinoflagellate *K. brevis* is the primary producer of PbTx and its response to OA has been studied. Elevated  $\text{pCO}_2$  had no significant effect on the cellular PbTx content of *K. brevis* [106,107]. Although *K. brevis* shifted its inorganic carbon preference from  $\text{HCO}_3^-$  to  $\text{CO}_2$  and the half-saturation constant ( $K_{1/2}$ ) for  $\text{CO}_2$  increased under high  $\text{CO}_2$  treatment, the growth rate, carbon fixation rate, and cellular carbon composition remained largely unchanged [106]. The relative insensitivity of *K. brevis* to elevated  $\text{pCO}_2$  was surprising as high  $\text{CO}_2$  availability had been thought to be especially beneficial to dinoflagellates that possess inefficient type II Rubisco [109].

### 3.2. OA May Affect the Central Carbon Metabolism of Toxic Microalgae

Based on the above, OA can affect the toxicity of some species of dinoflagellate *Alexandrium* and diatom *Pseudo-nitzschia*. On the other hand, dinoflagellate *K. brevis* was shown to be somewhat more resistant to OA and its toxicity was largely unchanged. The way in which they regulate central carbon metabolism under OA is likely to contribute to the changes in toxicity or to help to achieve homeostasis. OA was shown to be beneficial to *P. fraudulenta* as it promoted the carbon fixation rate by increasing inorganic carbon availability [103]. The increased growth rate and cellular toxin content gave rise to the hypothesis that excess carbon not used for growth might be shunted for toxin biosynthesis [99]. However, the positive relationship between the carbon fixation rate and toxin level does not always apply, as observed in *P. multiseriis* [104]. All biomolecules are carbon-based, so the excess fixed carbon is not necessarily transported for toxin production. The detailed routes of carbon reallocation for toxin biosynthesis have not been elucidated either. Therefore, investigating the central carbon metabolism of *Alexandrium* and *Pseudo-nitzschia* is important to validate the hypothesis. For *K. brevis*, the acquisition of inorganic carbon was shown to be affected by OA despite the nearly unchanged growth rate, carbon fixation rate, and toxin content [106]. Since central carbon metabolism is highly conserved across phylogeny [132], comparing the central carbon metabolism of relatively resistant *K. brevis* to that of other sensitive microalgae at elevated  $\text{pCO}_2$  may help to explain the unique response of *K. brevis* to OA. A decreased pH was proposed to affect the toxicity of *Pseudo-nitzschia*, though the exact mechanisms had not been demonstrated [119]. Increased inorganic carbon

availability and decreased pH may have combined effects on the regulation of central carbon metabolism in microalgae, hence affecting toxin biosynthesis. Considering the above, studying the carbon fluxes in *Alexandrium*, *Pseudo-nitzschia*, and *K. brevis* is essential to deepen our understanding of the effects of OA on microalgae.

#### 4. Future Research Directions

Manipulating seawater to a range of increased pCO<sub>2</sub> levels for OA experiments is not a straightforward task due to the interdependency of ocean carbon system components [133]. To predict the microalgal responses under OA accurately, the seawater used for microalgae cultivation should resemble the ocean carbon chemistry in future high CO<sub>2</sub> scenarios as closely as possible. Multiple seawater manipulation methods with distinct advantages and disadvantages have been applied to OA experiments. Most of the reviewed studies adopted CO<sub>2</sub> gas bubbling to model OA (Table 1). CO<sub>2</sub> gas bubbling is an efficient seawater manipulation method that exactly mimics the carbon chemistry of the ocean in future high atmospheric CO<sub>2</sub> scenarios (increased DIC without altering A<sub>T</sub>) [134]. In addition, it is easy to implement and it can maintain the initial conditions in the long term [135]. Thus, CO<sub>2</sub> gas bubbling was adopted by most of the studies to investigate the effects of OA on microalgae. However, the turbulence induced by bubbling may affect the growth of phytoplankton to a different extent, especially *Alexandrium spp.* [136]. Hence, the effects of turbulence became an uncontrolled confounding variable, which increased the difficulties in generating reproducible results for the microalgal adaptive response to OA [137]. To minimize the effects of turbulence, a dialysis bag with a 3 kDa molecular weight cut-off should be used to enclose the microalgae, so as to reduce the mechanical disturbance introduced by the aeration [135]. Unfortunately, none of the reviewed studies mentioned the uses of dialysis bags in their methodology. Besides CO<sub>2</sub> gas bubbling, mixing CO<sub>2</sub>-enriched water prior to cell inoculation, and the combined addition of HCl and Na<sub>2</sub>CO<sub>3</sub>/NaHCO<sub>3</sub>, are other seawater manipulation methods that also closely resemble the carbon chemistry of the ocean in future high atmospheric CO<sub>2</sub> conditions [134,135]. These methods can be effective and reliable alternatives to CO<sub>2</sub> gas bubbling without the mechanical disturbance to microalgae. Thus, they are especially useful for studying the effects of OA on microalgae with high sensitivity to turbulence. Regardless of the method used, it is noteworthy that the biological processes of microalgae, such as respiration and photosynthesis, will affect the carbon chemistry of seawater, especially when the biomass is high [138,139]. Thus, it would be preferable to monitor at least two carbon chemistry parameters of pH, A<sub>T</sub>, DIC, and pCO<sub>2</sub>, in addition to temperature and salinity, throughout the experiments [140].

With appropriate methods to model OA and monitor the carbon chemistry of the seawater, metabolomics is a useful technique to investigate the metabolic changes of the microalgae in response to OA. This will help to reveal the biological regulation of toxin biosynthesis in microalgae under OA. Metabolomics is the investigation of a complete set of small molecules with molecular weights lower than 1500 Da, also known as the metabolome, of biological samples [141]. It has been increasingly applied in algal toxin research with technological advancements [142,143]. Metabolic flux analysis (MFA) is an effective metabolomic tool that examines the turnover rate of metabolites by using stable isotope tracers such as <sup>13</sup>C, <sup>2</sup>H, and <sup>15</sup>N [144]. With the help of nuclear magnetic resonance (NMR) or mass spectrometry (MS), the isotope labeling patterns of intracellular metabolites are determined, which helps to construct a flux map, including reverse fluxes [145]. Compared to the measurement of metabolite levels, analyzing metabolic fluxes is more informative as it reveals the production and consumption rates of metabolites, which illustrate the biochemical events behind the changes in metabolite levels [146]. Based on the reviewed studies, it is hypothesized that the central carbon metabolism of toxic microalgae may be regulated differently under OA. The altered central carbon metabolism may then affect the toxicity of microalgae or relieve the stress brought by OA. Therefore, further studies on the central carbon metabolism of toxic microalgae are warranted. MFA has been applied for the investigation of photosynthesis and central carbon metabolism in

microalgae,  $C_3$ , and  $C_4$  plants recently in  $^{13}CO_2$  pulse labeling, and the distinct carbon flux pattern of microalgae has been successfully identified [147]. In this light, carbon allocation in toxic microalgae can be investigated to reveal the metabolic pathways related to toxin biosynthesis and their regulation under OA by MFA in order to elucidate the underlying mechanisms of toxicity changes. When conducting MFA to study the effects of OA on the carbon allocations of microalgae, it is critical to note that  $CO_2$  gas bubbling without the continuous control of the pH would alter the  $pCO_2$ , DIC, and pH of the seawater at the same time. As a result, it is difficult to determine which confounding variable causes the observed effects. Although  $CO_2$  gas bubbling successfully mimics the carbon chemistry of seawater under OA observed in reality, this method fails to decouple different variables in the carbon chemistry to study the individual effects of the variables on the carbon allocations of microalgae. Therefore, other methods or systems that can decouple different variables of the carbon chemistry of seawater under OA should also be adopted to investigate in detail the biological mechanisms of the changes in carbon allocation of microalgae under OA when using the metabolomic approach (Figure 1) [148].

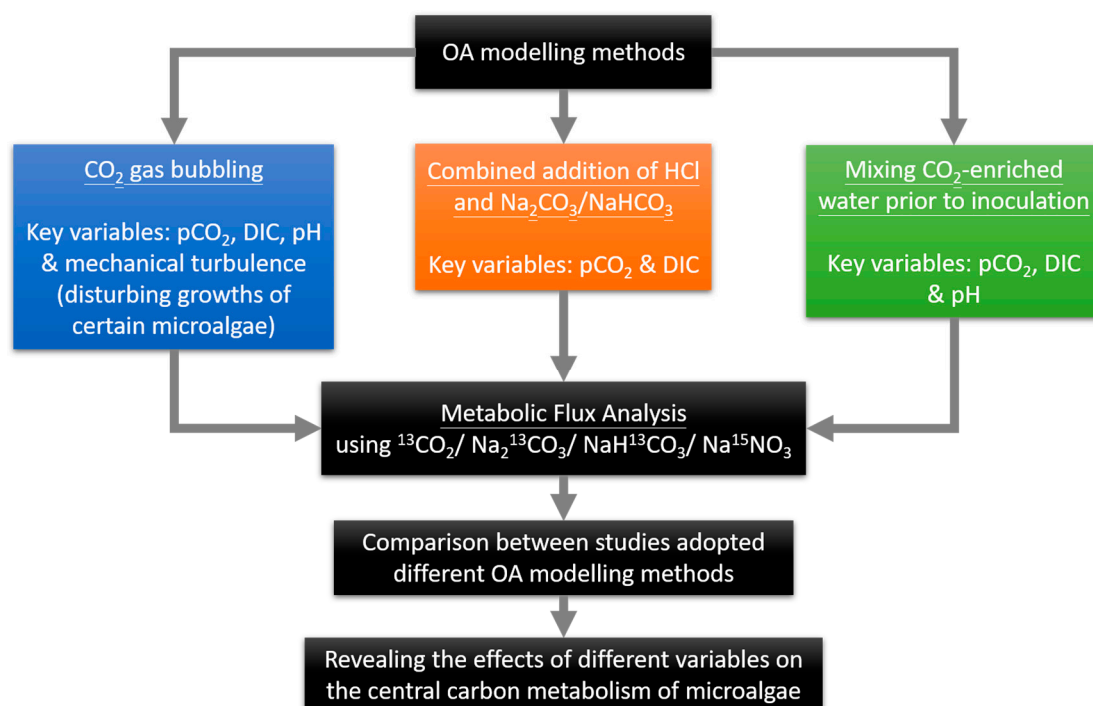


**Figure 1.** Schematic diagram illustrating the use of metabolomics to elucidate the individual effects of confounding factors on the carbon allocation of microalgae.

Knowledge of the relationship between environmental drivers and HABs is of fundamental importance to optimize the current mitigation of HABs [149]. Under climate change, it is undoubted that the HAB dynamic has been altered [1]. However, the physiological responses of toxigenic microalgae in changed climate conditions have not been well documented. A precise linkage between environmental factors and microalgal toxicity has not been confirmed due to the diverse responses displayed by microalgae belonging to the same genus or even the same species, as in the case of the STX-producing dinoflagellate *Alexandrium* [97–101,150]. MFA of the central carbon metabolism of microalgae can reveal the metabolic pathways that are responsible for the toxicity changes under OA. The identification of differentially regulated pathways will facilitate the discovery of universal biomarkers for potentially more toxic microalgae in future elevated atmospheric  $CO_2$  scenarios. Given the diverse responses of microalgae to different environmental conditions, detecting universal biomarkers is a relatively efficient way to identify microalgae with increased toxicity under climate change. Monitoring and forecasting these microalgae can be

prioritized to help establish early warning systems for the coastal tourism and aquaculture sectors, to minimize the economic losses caused by HABs [151–153]. Policymakers can guide the closure of beaches, fish farms, and shellfish-harvesting areas in an appropriate timeframe according to the early warning system, to protect public health while minimizing economic losses. Moreover, more research efforts can be implemented to understand the interactions between the potentially more toxic microalgae and other organisms in the food web under climate pressure. The findings can be used to assess the ecological risk of HABs in the future, which will aid policymakers to achieve a balance between environmental protection and economic development.

**Author Contributions:** Conceptualization: H.-K.K.; writing—original draft preparation, T.-K.V.T. and H.-K.K.; supervision: H.-K.K.; project administration: H.-K.K.; funding acquisition: H.-K.K. All authors have read and agreed to the published version of the manuscript.

**Funding:** This study was supported by research grants from the Hong Kong Polytechnic University (A/C: 1-BD8F) and the Research Grants Council (Ref. No.: 15102122).

**Institutional Review Board Statement:** Not applicable.

**Informed Consent Statement:** Not applicable.

**Data Availability Statement:** No new data were created or analyzed in this study. Data sharing is not applicable to this article.

**Conflicts of Interest:** The authors declare no conflict of interest.

## References

1. IPCC. *IPCC Special Report on the Ocean and Cryosphere in a Changing Climate*; Cambridge University Press: Cambridge, UK; New York, NY, USA, 2019.
2. Lopez, C.; Jewett, E.; Dortch, Q.; Walton, B.; Hudnell, H. *Scientific Assessment of Freshwater Harmful Algal Blooms*; Interagency Working Group on Harmful Algal Blooms, Hypoxia, and Human Health of the Joint Subcommittee on Ocean Science and Technology: Washington, DA, USA, 2008.
3. Gerssen, A.; Pol-Hofstad, I.E.; Poelman, M.; Mulder, P.P.; van den Top, H.J.; de Boer, J. Marine toxins: Chemistry, toxicity, occurrence and detection, with special reference to the Dutch situation. *Toxins* **2010**, *2*, 878–904. [[CrossRef](#)] [[PubMed](#)]
4. Van Dolah, F.M. Marine algal toxins: Origins, health effects, and their increased occurrence. *Environ. Health Perspect.* **2000**, *108* (Suppl. S1), 133–141. [[CrossRef](#)]
5. Wang, D.Z. Neurotoxins from marine dinoflagellates: A brief review. *Mar. Drugs* **2008**, *6*, 349–371. [[CrossRef](#)] [[PubMed](#)]
6. Kouakou, C.R.C.; Poder, T.G. Economic impact of harmful algal blooms on human health: A systematic review. *J. Water Health* **2019**, *17*, 499–516. [[CrossRef](#)] [[PubMed](#)]
7. Park, T.G.; Lim, W.A.; Park, Y.T.; Lee, C.K.; Jeong, H.J. Economic impact, management and mitigation of red tides in Korea. *Harmful Algae* **2013**, *30*, S131–S143. [[CrossRef](#)]
8. Larkin, S.L.; Adams, C.M.; Ballyram, D.M.; Hodges, A. Red tides and coastal businesses: Measuring economic consequences in Florida. *Soc. Nat. Resour.* **2007**, *20*, 2007. [[CrossRef](#)]
9. Sanseverino, I.; Conduto, D.; Pozzoli, L.; Dobricic, S.; Lettieri, T. *Algal bloom and its economic impact*; Publications Office of the European Union: Luxembourg, 2016. [[CrossRef](#)]
10. Gobler, C.J. Climate Change and Harmful Algal Blooms: Insights and perspective. *Harmful Algae* **2020**, *91*, 101731. [[CrossRef](#)]
11. Moore, S.K.; Trainer, V.L.; Mantua, N.J.; Parker, M.S.; Laws, E.A.; Backer, L.C.; Fleming, L.E. Impacts of climate variability and future climate change on harmful algal blooms and human health. In Proceedings of the Centers for Oceans and Human Health Investigators Meeting, Woods Hole, MA, USA, 24–27 April 2007; p. S4.
12. Wells, M.L.; Karlson, B.; Wulff, A.; Kudela, R.; Trick, C.; Asnaghi, V.; Berdalet, E.; Cochlan, W.; Davidson, K.; De Rijcke, M.; et al. Future HAB science: Directions and challenges in a changing climate. *Harmful Algae* **2020**, *91*, 101632. [[CrossRef](#)]
13. Wells, M.L.; Trainer, V.L.; Smayda, T.J.; Karlson, B.S.; Trick, C.G.; Kudela, R.M.; Ishikawa, A.; Bernard, S.; Wulff, A.; Anderson, D.M.; et al. Harmful algal blooms and climate change: Learning from the past and present to forecast the future. *Harmful Algae* **2015**, *49*, 68–93. [[CrossRef](#)]
14. Griffith, A.W.; Gobler, C.J. Harmful algal blooms: A climate change co-stressor in marine and freshwater ecosystems. *Harmful Algae* **2020**, *91*, 101590. [[CrossRef](#)]
15. Kazmi, S.S.U.H.; Yapa, N.; Karunarathna, S.C.; Suwannarach, N. Perceived Intensification in Harmful Algal Blooms Is a Wave of Cumulative Threat to the Aquatic Ecosystems. *Biology* **2022**, *11*, 852. [[CrossRef](#)]
16. Hallegraeff, G.; Enevoldsen, H.; Zingone, A.; Schweibold, L.; De Rijcke, M. *GLOBAL Harmful Algal Bloom Status Report 2021*; UNESCO: Paris, France, 2021.

17. Wiese, M.; D'Agostino, P.M.; Mihali, T.K.; Moffitt, M.C.; Neilan, B.A. Neurotoxic alkaloids: Saxitoxin and its analogs. *Mar. Drugs* **2010**, *8*, 2185–2211. [[CrossRef](#)] [[PubMed](#)]
18. Schantz, E.J.; Ghazarossian, V.E.; Schnoes, H.K.; Strong, F.M.; Springer, J.P.; Pezzanite, J.O.; Clardy, J. Letter: The structure of saxitoxin. *J. Am. Chem. Soc.* **1975**, *97*, 1238. [[CrossRef](#)] [[PubMed](#)]
19. Oshima, Y.; Blackburn, S.; Hallegraef, G. Comparative study on paralytic shellfish toxin profiles of the dinoflagellate *Gymnodinium catenatum* from three different countries. *Mar. Biol.* **1993**, *116*, 471–476. [[CrossRef](#)]
20. Usup, G.; Kulis, D.M.; Anderson, D.M. Growth and toxin production of the toxic dinoflagellate *Pyrodinium bahamense* var. *compressum* in laboratory cultures. *Nat. Toxins* **1994**, *2*, 254–262. [[CrossRef](#)]
21. Carmichael, W.W.; Evans, W.R.; Yin, Q.Q.; Bell, P.; Moczydlowski, E. Evidence for paralytic shellfish poisons in the freshwater cyanobacterium *Lyngbya wollei* (Farlow ex Gomont) comb. nov. *Appl. Environ. Microbiol.* **1997**, *63*, 3104–3110. [[CrossRef](#)]
22. Hoeger, S.J.; Shaw, G.; Hitzfeld, B.C.; Dietrich, D.R. Occurrence and elimination of cyanobacterial toxins in two Australian drinking water treatment plants. *Toxicon* **2004**, *43*, 639–649. [[CrossRef](#)] [[PubMed](#)]
23. Liu, Y.; Chen, W.; Li, D.; Shen, Y.; Li, G.; Liu, Y. First report of aphantoxins in China—waterblooms of toxigenic *Aphanizomenon flos-aquae* in Lake Dianchi. *Ecotoxicol. Environ. Saf.* **2006**, *65*, 84–92. [[CrossRef](#)]
24. Pomati, F.; Sacchi, S.; Rossetti, C.; Giovannardi, S.; Onodera, H.; Oshima, Y.; Neilan, B.A. The Freshwater Cyanobacterium *Planktothrix* Sp. Fp1: Molecular Identification and Detection of Paralytic Shellfish Poisoning Toxins. *J. Phycol.* **2000**, *36*, 553–562. [[CrossRef](#)]
25. Cestele, S.; Catterall, W.A. Molecular mechanisms of neurotoxin action on voltage-gated sodium channels. *Biochimie* **2000**, *82*, 883–892. [[CrossRef](#)]
26. Llewellyn, L.E. Saxitoxin, a toxic marine natural product that targets a multitude of receptors. *Nat. Prod. Rep.* **2006**, *23*, 200–222. [[CrossRef](#)] [[PubMed](#)]
27. Deeds, J.R.; Landsberg, J.H.; Etheridge, S.M.; Pitcher, G.C.; Longan, S.W. Non-traditional vectors for paralytic shellfish poisoning. *Mar. Drugs* **2008**, *6*, 308–348. [[CrossRef](#)] [[PubMed](#)]
28. Klemm, K.; Cembella, A.; Clarke, D.; Cusack, C.; Arneborg, L.; Karlson, B.; Liu, Y.; Naustvoll, L.; Siano, R.; Gran-Stadniczenko, S.; et al. Apparent biogeographical trends in *Alexandrium* blooms for northern Europe: Identifying links to climate change and effective adaptive actions. *Harmful Algae* **2022**, *119*, 102335. [[CrossRef](#)] [[PubMed](#)]
29. Schweibold, L. *Global Status of Harmful Algal Blooms: First Steps of a Metadata Approach*; ResearchGate: Berlin, Germany, 2017. [[CrossRef](#)]
30. Liu, M.; Zheng, J.; Krock, B.; Ding, G.; MacKenzie, L.; Smith, K.F.; Gu, H. Dynamics of the Toxic Dinoflagellate *Alexandrium pacificum* in the Taiwan Strait and Its Linkages to Surrounding Populations. *Water* **2021**, *13*, 2681. [[CrossRef](#)]
31. Selina, M.; Konovalova, G.; Morozova, T.; Orlova, T.Y. Genus *Alexandrium* Halim, 1960 (Dinophyta) from the Pacific coast of Russia: Species composition, distribution, and dynamics. *Russ. J. Mar. Biol.* **2006**, *32*, 321–332. [[CrossRef](#)]
32. Anderson, D.M.; Fachon, E.; Pickart, R.S.; Lin, P.; Fischer, A.D.; Richlen, M.L.; Uva, V.; Brosnahan, M.L.; McRaven, L.; Bahr, F.; et al. Evidence for massive and recurrent toxic blooms of *Alexandrium catenella* in the Alaskan Arctic. *Proc. Natl. Acad. Sci. USA* **2021**, *118*, e2107387118. [[CrossRef](#)] [[PubMed](#)]
33. Egmond, H.P.; Van Apeldoorn, M. *Marine Biotoxins*; Food & Agriculture Organization: Rome, Italy, 2004.
34. Hamano, Y.; Kinoshita, Y.; Yasumoto, T. Enteropathogenicity of Diarrhetic Shellfish Toxins in Intestinal Models Studies on Diarrhetic Shellfish Toxins. I. *Food Hyg. Saf. Sci. (Shokuhin Eiseigaku Zasshi)* **1986**, *27*, 375–379\_1. [[CrossRef](#)]
35. FAO. *Toxicity Equivalence Factors for Marine Biotoxins Associated with Bivalve Molluscs*; World Health Organization: Geneva, Switzerland, 2016.
36. WHO. *Aquatic (Marine and Freshwater) Biotoxins-Environmental Health Criteria 37*; WHO: Geneva, Switzerland, 1984.
37. Reboreda, A.; Lago, J.; Chapela, M.J.; Vieites, J.M.; Botana, L.M.; Alfonso, A.; Cabado, A.G. Decrease of marine toxin content in bivalves by industrial processes. *Toxicon* **2010**, *55*, 235–243. [[CrossRef](#)]
38. Dounay, A.B.; Forsyth, C.J. Okadaic acid: The archetypal serine/threonine protein phosphatase inhibitor. *Curr. Med. Chem.* **2002**, *9*, 1939–1980. [[CrossRef](#)]
39. Takai, A.; Murata, M.; Torigoe, K.; Isobe, M.; Mieskes, G.; Yasumoto, T. Inhibitory effect of okadaic acid derivatives on protein phosphatases. A study on structure-affinity relationship. *Biochem. J.* **1992**, *284 Pt 2*, 539–544. [[CrossRef](#)]
40. Wang, J.; Wang, Y.Y.; Lin, L.; Gao, Y.; Hong, H.S.; Wang, D.Z. Quantitative proteomic analysis of okadaic acid treated mouse small intestines reveals differentially expressed proteins involved in diarrhetic shellfish poisoning. *J. Proteomics* **2012**, *75*, 2038–2052. [[CrossRef](#)] [[PubMed](#)]
41. Falconer, I.R. *Algal toxins in seafood and drinking water*; Elsevier: Amsterdam, The Netherlands, 2012.
42. Heil, C.A.; Glibert, P.M.; Fan, C. *Prorocentrum minimum* (Pavillard) Schiller. *Harmful Algae* **2005**, *4*, 449–470. [[CrossRef](#)]
43. Edwards, M.; Johns, D.; Leterme, S.; Svendsen, E.; Richardson, A. Regional climate change and harmful algal blooms in the northeast Atlantic. *Limnol. Oceanogr.* **2006**, *51*, 820–829. [[CrossRef](#)]
44. Bates, S.S.; Hubbard, K.A.; Lundholm, N.; Montresor, M.; Leaw, C.P. Pseudo-nitzschia, Nitzschia, and domoic acid: New research since 2011. *Harmful Algae* **2018**, *79*, 3–43. [[CrossRef](#)] [[PubMed](#)]

45. Steele, T.S.; Brunson, J.K.; Maeno, Y.; Terada, R.; Allen, A.E.; Yotsu-Yamashita, M.; Chekan, J.R.; Moore, B.S. Domoic acid biosynthesis in the red alga *Chondria armata* suggests a complex evolutionary history for toxin production. *Proc. Natl. Acad. Sci. USA* **2022**, *119*, e2117407119. [[CrossRef](#)] [[PubMed](#)]
46. Wright, J.; Boyd, R.; Freitas, A.d.; Falk, M.; Foxall, R.; Jamieson, W.; Laycock, M.; McCulloch, A.; McInnes, A.; Odense, P. Identification of domoic acid, a neuroexcitatory amino acid, in toxic mussels from eastern Prince Edward Island. *Can. J. Chem.* **1989**, *67*, 481–490. [[CrossRef](#)]
47. de la Iglesia, P.; Gimenez, G.; Diogene, J. Determination of dissolved domoic acid in seawater with reversed-phase extraction disks and rapid resolution liquid chromatography tandem mass spectrometry with head-column trapping. *J. Chromatogr. A* **2008**, *1215*, 116–124. [[CrossRef](#)]
48. Berman, F.W.; Murray, T.F. Domoic acid neurotoxicity in cultured cerebellar granule neurons is mediated predominantly by NMDA receptors that are activated as a consequence of excitatory amino acid release. *J. Neurochem.* **1997**, *69*, 693–703. [[CrossRef](#)]
49. Larm, J.A.; Beart, P.M.; Cheung, N.S. Neurotoxin domoic acid produces cytotoxicity via kainate- and AMPA-sensitive receptors in cultured cortical neurones. *Neurochem. Int.* **1997**, *31*, 677–682. [[CrossRef](#)]
50. Pinheiro, P.; Mulle, C. Kainate receptors. *Cell Tissue Res.* **2006**, *326*, 457–482. [[CrossRef](#)]
51. Paoletti, P.; Neyton, J. NMDA receptor subunits: Function and pharmacology. *Curr. Opin. Pharmacol.* **2007**, *7*, 39–47. [[CrossRef](#)]
52. Carcache, L.M.; Rodriguez, J.; Rein, K.S. The structural basis for kainoid selectivity at AMPA receptors revealed by low-mode docking calculations. *Bioorganic Med. Chem.* **2003**, *11*, 551–559. [[CrossRef](#)] [[PubMed](#)]
53. Hampson, D.R.; Manalo, J.L. The activation of glutamate receptors by kainic acid and domoic acid. *Nat. Toxins* **1998**, *6*, 153–158. [[CrossRef](#)]
54. Colman, J.R.; Nowocin, K.J.; Switzer, R.C.; Trusk, T.C.; Ramsdell, J.S. Mapping and reconstruction of domoic acid-induced neurodegeneration in the mouse brain. *Neurotoxicol. Teratol.* **2005**, *27*, 753–767. [[CrossRef](#)]
55. Giordano, G.; Klintworth, H.M.; Kavanagh, T.J.; Costa, L.G. Apoptosis induced by domoic acid in mouse cerebellar granule neurons involves activation of p38 and JNK MAP kinases. *Neurochem. Int.* **2008**, *52*, 1100–1105. [[CrossRef](#)]
56. Pulido, O.M. Domoic acid toxicologic pathology: A review. *Mar. Drugs* **2008**, *6*, 180–219. [[CrossRef](#)] [[PubMed](#)]
57. Perl, T.M.; Bedard, L.; Kosatsky, T.; Hockin, J.C.; Todd, E.C.; Remis, R.S. An outbreak of toxic encephalopathy caused by eating mussels contaminated with domoic acid. *N. Engl. J. Med* **1990**, *322*, 1775–1780. [[CrossRef](#)] [[PubMed](#)]
58. Munday, R.; Holland, P.T.; McNabb, P.; Selwood, A.I.; Rhodes, L.L. Comparative toxicity to mice of domoic acid and isodomoic acids A, B and C. *Toxicon* **2008**, *52*, 954–956. [[CrossRef](#)] [[PubMed](#)]
59. Sawant, P.M.; Tyndall, J.D.; Holland, P.T.; Peake, B.M.; Mountfort, D.O.; Kerr, D.S. In vivo seizure induction and affinity studies of domoic acid and isodomoic acids-D, -E and -F. *Neuropharmacology* **2010**, *59*, 129–138. [[CrossRef](#)]
60. Sawant, P.M.; Weare, B.A.; Holland, P.T.; Selwood, A.I.; King, K.L.; Mikulski, C.M.; Doucette, G.J.; Mountfort, D.O.; Kerr, D.S. Isodomoic acids A and C exhibit low KA receptor affinity and reduced in vitro potency relative to domoic acid in region CA1 of rat hippocampus. *Toxicon* **2007**, *50*, 627–638. [[CrossRef](#)] [[PubMed](#)]
61. Silver, M.W.; Bargu, S.; Coale, S.L.; Benitez-Nelson, C.R.; Garcia, A.C.; Roberts, K.J.; Sekula-Wood, E.; Bruland, K.W.; Coale, K.H. Toxic diatoms and domoic acid in natural and iron enriched waters of the oceanic Pacific. *Proc. Natl. Acad. Sci. USA* **2010**, *107*, 20762–20767. [[CrossRef](#)]
62. Landsberg, J.H.; Flewelling, L.J.; Naar, J. *Karenia brevis* red tides, brevetoxins in the food web, and impacts on natural resources: Decadal advancements. *Harmful Algae* **2009**, *8*, 598–607. [[CrossRef](#)]
63. Bourdelais, A.J.; Tomas, C.R.; Naar, J.; Kubanek, J.; Baden, D.G. New fish-killing alga in coastal Delaware produces neurotoxins. *Environ. Health Perspect.* **2002**, *110*, 465–470. [[CrossRef](#)] [[PubMed](#)]
64. Baden, D.G.; Bourdelais, A.J.; Jacocks, H.; Michelliza, S.; Naar, J. Natural and derivative brevetoxins: Historical background, multiplicity, and effects. *Environ. Health Perspect.* **2005**, *113*, 621–625. [[CrossRef](#)]
65. Ramsdell, J. The Molecular and Integrative Basis to Brevetoxin Toxicity. In *Seafood and Freshwater Toxins*; Food Science and Technology; Taylor & Francis Group: Boca Raton, FL, USA, 2008; pp. 519–550.
66. Konoki, K.; Baden, D.G.; Scheuer, T.; Catterall, W.A. Molecular Determinants of Brevetoxin Binding to Voltage-Gated Sodium Channels. *Toxins* **2019**, *11*, 513. [[CrossRef](#)]
67. Morris, P.D.; Campbell, D.S.; Taylor, T.J.; Freeman, J.I. Clinical and epidemiological features of neurotoxic shellfish poisoning in North Carolina. *Am. J. Public Health* **1991**, *81*, 471–474. [[CrossRef](#)]
68. Steidinger, K.A. Historical perspective on *Karenia brevis* red tide research in the Gulf of Mexico. *Harmful Algae* **2009**, *8*, 549–561. [[CrossRef](#)]
69. Watkins, S.M.; Reich, A.; Fleming, L.E.; Hammond, R. Neurotoxic shellfish poisoning. *Mar. Drugs* **2008**, *6*, 431–455. [[CrossRef](#)]
70. Tillmann, U. Amphidomataceae. In *Harmful Algae Blooms, a Compendium Desk Reference*; Wiley-Blackwell Publishing: Chichester, West Sussex, 2018; pp. 575–582.
71. Satake, M.; Ofuji, K.; Naoki, H.; James, K.J.; Furey, A.; McMahon, T.; Silke, J.; Yasumoto, T. Azaspiracid, a new marine toxin having unique spiro ring assemblies, isolated from Irish mussels, *Mytilus edulis*. *J. Am. Chem. Soc.* **1998**, *120*, 9967–9968. [[CrossRef](#)]
72. Krock, B.; Tillmann, U.; Tebben, J.; Trefault, N.; Gu, H. Two novel azaspiracids from *Azadinium poporum*, and a comprehensive compilation of azaspiracids produced by Amphidomataceae, (Dinophyceae). *Harmful Algae* **2019**, *82*, 1–8. [[CrossRef](#)] [[PubMed](#)]

73. Twiner, M.J.; Rehmman, N.; Hess, P.; Doucette, G.J. Azaspiracid shellfish poisoning: A review on the chemistry, ecology, and toxicology with an emphasis on human health impacts. *Mar. Drugs* **2008**, *6*, 39–72. [[CrossRef](#)] [[PubMed](#)]
74. Furey, A.; O'Doherty, S.; O'Callaghan, K.; Lehane, M.; James, K.J. Azaspiracid poisoning (AZP) toxins in shellfish: Toxicological and health considerations. *Toxicon* **2010**, *56*, 173–190. [[CrossRef](#)] [[PubMed](#)]
75. Twiner, M.J.; Doucette, G.J.; Rasky, A.; Huang, X.P.; Roth, B.L.; Sanguinetti, M.C. Marine algal toxin azaspiracid is an open-state blocker of hERG potassium channels. *Chem. Res. Toxicol.* **2012**, *25*, 1975–1984. [[CrossRef](#)]
76. Tillmann, U.; Edvardsen, B.; Krock, B.; Smith, K.F.; Paterson, R.F.; Voss, D. Diversity, distribution, and azaspiracids of Amphidomataceae (Dinophyceae) along the Norwegian coast. *Harmful Algae* **2018**, *80*, 15–34. [[CrossRef](#)]
77. McGirr, S.; Clarke, D.; Kilcoyne, J.; Silke, J.; Touzet, N. Co-localisation of Azaspiracid Analogs with the Dinoflagellate Species *Azadinium spinosum* and *Amphidoma languida* in the Southwest of Ireland. *Microb. Ecol.* **2022**, *83*, 635–646. [[CrossRef](#)]
78. Akselman, R.; Negri, R.M. Blooms of *Azadinium* cf. *spinosum* Elbrächter et Tillmann (Dinophyceae) in northern shelf waters of Argentina, Southwestern Atlantic. *Harmful Algae* **2012**, *19*, 30–38. [[CrossRef](#)]
79. Percopo, I.; Siano, R.; Rossi, R.; Soprano, V.; Sarno, D.; Zingone, A. A new potentially toxic *Azadinium* species (Dinophyceae) from the Mediterranean Sea, *A. dexteroporum* sp. nov. *J. Phycol.* **2013**, *49*, 950–966. [[CrossRef](#)]
80. Gu, H.; Luo, Z.; Krock, B.; Witt, M.; Tillmann, U. Morphology, phylogeny and azaspiracid profile of *Azadinium poporum* (Dinophyceae) from the China Sea. *Harmful Algae* **2013**, *21–22*, 64–75. [[CrossRef](#)]
81. Kim, J.H.; Tillmann, U.; Adams, N.G.; Krock, B.; Stutts, W.L.; Deeds, J.R.; Han, M.S.; Trainer, V.L. Identification of *Azadinium* species and a new azaspiracid from *Azadinium poporum* in Puget Sound, Washington State, USA. *Harmful Algae* **2017**, *68*, 152–167. [[CrossRef](#)]
82. Tillmann, U.; Trefault, N.; Krock, B.; Parada-Pozo, G.; De la Iglesia, R.; Vásquez, M. Identification of *Azadinium poporum* (Dinophyceae) in the Southeast Pacific: Morphology, molecular phylogeny, and azaspiracid profile characterization. *J. Plankton Res.* **2017**, *39*, 350–367. [[CrossRef](#)]
83. Tillmann, U.; Jaen, D.; Fernandez, L.; Gottschling, M.; Witt, M.; Blanco, J.; Krock, B. *Amphidoma languida* (Amphidomatacea, Dinophyceae) with a novel azaspiracid toxin profile identified as the cause of molluscan contamination at the Atlantic coast of southern Spain. *Harmful Algae* **2017**, *62*, 113–126. [[CrossRef](#)]
84. Wietkamp, S.; Tillmann, U.; Clarke, D.; Toebe, K. Molecular detection and quantification of the azaspiracid-producing dinoflagellate *Amphidoma languida* (Amphidomataceae, Dinophyceae). *J. Plankton Res.* **2019**, *41*, 101–113. [[CrossRef](#)]
85. Keeling, C.D.; Piper, S.C.; Bacastow, R.B.; Wahlen, M.; Whorf, T.P.; Heimann, M.; Meijer, H.A. *Exchanges of Atmospheric CO<sub>2</sub> and 13CO<sub>2</sub> with the Terrestrial Biosphere and Oceans from 1978 to 2000. I. Global Aspects*; Springer: New York, NY, USA, 2001.
86. IPCC. *Climate Change 2014: Synthesis Report*; IPCC: Geneva, Switzerland, 2014; p. 151.
87. Sabine, C.L.; Feely, R.A.; Gruber, N.; Key, R.M.; Lee, K.; Bullister, J.L.; Wanninkhof, R.; Wong, C.S.; Wallace, D.W.; Tilbrook, B.; et al. The oceanic sink for anthropogenic CO<sub>2</sub>. *Science* **2004**, *305*, 367–371. [[CrossRef](#)] [[PubMed](#)]
88. Kroeker, K.J.; Kordas, R.L.; Crim, R.N.; Singh, G.G. Meta-analysis reveals negative yet variable effects of ocean acidification on marine organisms. *Ecol. Lett.* **2010**, *13*, 1419–1434. [[CrossRef](#)]
89. Al Jabri, H.; Taleb, A.; Touchard, R.; Saadaoui, I.; Goetz, V.; Pruvost, J. Cultivating Microalgae in Desert Conditions: Evaluation of the Effect of Light-Temperature Summer Conditions on the Growth and Metabolism of *Nannochloropsis* QU130. *Appl. Sci.* **2021**, *11*, 3799. [[CrossRef](#)]
90. Procházková, G.; Brányiková, I.; Zachleder, V.; Brányik, T. Effect of nutrient supply status on biomass composition of eukaryotic green microalgae. *J. Appl. Phycol.* **2013**, *26*, 1359–1377. [[CrossRef](#)]
91. Brand, L.E.; Campbell, L.; Bresnan, E. *Karenia*: The biology and ecology of a toxic genus. *Harmful Algae* **2012**, *14*, 156–178. [[CrossRef](#)]
92. Shearn-Bochsler, V.; Lance, E.W.; Corcoran, R.; Piatt, J.; Bodenstern, B.; Frame, E.; Lawonn, J. Fatal paralytic shellfish poisoning in Kittlitz's Murrelet (*Brachyramphus brevirostris*) nestlings, Alaska, USA. *J. Wildl. Dis.* **2014**, *50*, 933–937. [[CrossRef](#)]
93. Garcia, C.; Perez, F.; Contreras, C.; Figueroa, D.; Barriga, A.; Lopez-Rivera, A.; Araneda, O.F.; Contreras, H.R. Saxitoxins and okadaic acid group: Accumulation and distribution in invertebrate marine vectors from Southern Chile. *Food Addit. Contam. Part A Chem. Anal. Control. Expo. Risk Assess* **2015**, *32*, 984–1002. [[CrossRef](#)] [[PubMed](#)]
94. Bejarano, A.C.; VanDola, F.M.; Gulland, F.M.; Rowles, T.K.; Schwacke, L.H. Production and toxicity of the marine biotoxin domoic acid and its effects on wildlife: A review. *Hum. Ecol. Risk Assess.* **2008**, *14*, 544–567. [[CrossRef](#)]
95. Burkholder, J.M.; Shumway, S.E.; Glibert, P.M. Food web and ecosystem impacts of harmful algae. *Harmful Algal Bloom. A Compend. Desk Ref.* **2018**, 243–336.
96. Roggatz, C.C.; Fletcher, N.; Benoit, D.M.; Algar, A.C.; Doroff, A.; Wright, B.; Wollenberg Valero, K.C.; Hardege, J.D. Saxitoxin and tetrodotoxin bioavailability increases in future oceans. *Nat. Clim. Change* **2019**, *9*, 840–844. [[CrossRef](#)]
97. Hattenrath-Lehmann, T.K.; Smith, J.L.; Wallace, R.B.; Merlo, L.; Koch, F.; Mittelsdorf, H.; Goleski, J.A.; Anderson, D.M.; Gobler, C.J. The effects of elevated CO<sub>2</sub> on the growth and toxicity of field populations and cultures of the saxitoxin-producing dinoflagellate, *Alexandrium fundyense*. *Limnol Oceanogr* **2015**, *60*, 198–214. [[CrossRef](#)] [[PubMed](#)]
98. Lian, Z.; Li, F.; He, X.; Chen, J.; Yu, R.-C. Rising CO<sub>2</sub> will increase toxicity of marine dinoflagellate *Alexandrium minutum*. *J. Hazard. Mater.* **2022**, *431*, 128627. [[CrossRef](#)]

99. Tatters, A.O.; Flewelling, L.J.; Fu, F.; Granholm, A.A.; Hutchins, D.A. High CO<sub>2</sub> promotes the production of paralytic shellfish poisoning toxins by *Alexandrium catenella* from Southern California waters. *Harmful Algae* **2013**, *30*, 37–43. [[CrossRef](#)]
100. Brandenburg, K.M.; Krock, B.; Klip, H.C.L.; Sluijs, A.; Garbeva, P.; Van de Waal, D.B. Intraspecific variation in multiple trait responses of *Alexandrium ostenfeldii* towards elevated pCO<sub>2</sub>. *Harmful Algae* **2021**, *101*, 101970. [[CrossRef](#)] [[PubMed](#)]
101. Van de Waal, D.B.; Eberlein, T.; John, U.; Wohlrab, S.; Rost, B. Impact of elevated pCO<sub>2</sub> on paralytic shellfish poisoning toxin content and composition in *Alexandrium tamarense*. *Toxicon* **2014**, *78*, 58–67. [[CrossRef](#)]
102. Sun, J.; Hutchins, D.A.; Feng, Y.; Seubert, E.L.; Caron, D.A.; Fu, F.-X. Effects of changing pCO<sub>2</sub> and phosphate availability on domoic acid production and physiology of the marine harmful bloom diatom *Pseudo-nitzschia multiseries*. *Limnol. Oceanogr.* **2011**, *56*, 829–840. [[CrossRef](#)]
103. Tatters, A.O.; Fu, F.X.; Hutchins, D.A. High CO<sub>2</sub> and silicate limitation synergistically increase the toxicity of *Pseudo-nitzschia fraudulenta*. *PLoS ONE* **2012**, *7*, e32116. [[CrossRef](#)]
104. Wingert, C.J.; Cochlan, W.P. Effects of ocean acidification on the growth, photosynthetic performance, and domoic acid production of the diatom *Pseudo-nitzschia australis* from the California Current System. *Harmful Algae* **2021**, *107*, 102030. [[CrossRef](#)]
105. Wohlrab, S.; John, U.; Klemm, K.; Eberlein, T.; Forsberg Grivogiannis, A.M.; Krock, B.; Frickenhaus, S.; Bach, L.T.; Rost, B.; Riebesell, U.; et al. Ocean acidification increases domoic acid contents during a spring to summer succession of coastal phytoplankton. *Harmful Algae* **2020**, *92*, 101697. [[CrossRef](#)] [[PubMed](#)]
106. Berce, T.L.; Kranz, S.A. Insights into carbon acquisition and photosynthesis in *Karenia brevis* under a range of CO<sub>2</sub> concentrations. *Prog. Oceanogr.* **2019**, *172*, 65–76. [[CrossRef](#)]
107. Errera, R.M.; Yvon-Lewis, S.; Kessler, J.D.; Campbell, L. Responses of the dinoflagellate *Karenia brevis* to climate change: pCO<sub>2</sub> and sea surface temperatures. *Harmful Algae* **2014**, *37*, 110–116. [[CrossRef](#)]
108. Raven, J.A.; Cockell, C.S.; De La Rocha, C.L. The evolution of inorganic carbon concentrating mechanisms in photosynthesis. *Philos. Trans. R. Soc. Lond B. Biol. Sci.* **2008**, *363*, 2641–2650. [[CrossRef](#)] [[PubMed](#)]
109. Tortell, P.D. Evolutionary and ecological perspectives on carbon acquisition in phytoplankton. *Limnol. Oceanogr.* **2000**, *45*, 744–750. [[CrossRef](#)]
110. Kellmann, R.; Mihali, T.K.; Jeon, Y.J.; Pickford, R.; Pomati, F.; Neilan, B.A. Biosynthetic intermediate analysis and functional homology reveal a saxitoxin gene cluster in cyanobacteria. *Appl. Environ. Microbiol.* **2008**, *74*, 4044–4053. [[CrossRef](#)]
111. Taroncher-Oldenburg, G.; Anderson, D.M. Identification and characterization of three differentially expressed genes, encoding S-adenosylhomocysteine hydrolase, methionine aminopeptidase, and a histone-like protein, in the toxic dinoflagellate *Alexandrium fundyense*. *Appl. Environ. Microbiol.* **2000**, *66*, 2105–2112. [[CrossRef](#)]
112. Pang, M.; Xu, J.; Qu, P.; Mao, X.; Wu, Z.; Xin, M.; Sun, P.; Wang, Z.; Zhang, X.; Chen, H. Effect of CO<sub>2</sub> on growth and toxicity of *Alexandrium tamarense* from the East China Sea, a major producer of paralytic shellfish toxins. *Harmful Algae* **2017**, *68*, 240–247. [[CrossRef](#)] [[PubMed](#)]
113. Hackett, J.D.; Wisecaver, J.H.; Brosnahan, M.L.; Kulis, D.M.; Anderson, D.M.; Bhattacharya, D.; Plumley, F.G.; Erdner, D.L. Evolution of saxitoxin synthesis in cyanobacteria and dinoflagellates. *Mol. Biol. Evol.* **2013**, *30*, 70–78. [[CrossRef](#)] [[PubMed](#)]
114. Moustafa, A.; Loram, J.E.; Hackett, J.D.; Anderson, D.M.; Plumley, F.G.; Bhattacharya, D. Origin of saxitoxin biosynthetic genes in cyanobacteria. *PLoS ONE* **2009**, *4*, e5758. [[CrossRef](#)] [[PubMed](#)]
115. Sako, Y.; Yoshida, T.; Uchida, A.; Arakawa, O.; Noguchi, T.; Ishida, Y. Purification and characterization of a sulfotransferase specific to N-21 of saxitoxin and gonyautoxin 2+ 3 from the toxic dinoflagellate *Gymnodinium catenatum* (Dinophyceae). *J. Phycol.* **2001**, *37*, 1044–1051. [[CrossRef](#)]
116. Soto-Liebe, K.; Murillo, A.A.; Krock, B.; Stucken, K.; Fuentes-Valdes, J.J.; Trefault, N.; Cembella, A.; Vasquez, M. Reassessment of the toxin profile of *Cylindrospermopsis raciborskii* T3 and function of putative sulfotransferases in synthesis of sulfated and sulfonated PSP toxins. *Toxicon* **2010**, *56*, 1350–1361. [[CrossRef](#)]
117. Giordano, M.; Norici, A.; Hell, R. Sulfur and phytoplankton: Acquisition, metabolism and impact on the environment. *New Phytol.* **2005**, *166*, 371–382. [[CrossRef](#)] [[PubMed](#)]
118. Shibagaki, N.; Grossman, A. The state of sulfur metabolism in algae: From ecology to genomics. In *Sulfur Metabolism in Phototrophic Organisms*; Springer: Berlin/Heidelberg, Germany, 2008; pp. 231–267.
119. Lundholm, N.; Hansen, P.J.; Kotaki, Y. Effect of pH on growth and domoic acid production by potentially toxic diatoms of the genera *Pseudo-nitzschia* and *Nitzschia*. *Mar. Ecol. Prog. Ser.* **2004**, *273*, 1–15. [[CrossRef](#)]
120. Shi, D.; Hong, H.; Su, X.; Liao, L.; Chang, S.; Lin, W. The physiological response of marine diatoms to ocean acidification: Differential roles of seawater pCO<sub>2</sub> and pH. *J. Phycol.* **2019**, *55*, 521–533. [[CrossRef](#)] [[PubMed](#)]
121. Trimborn, S.; Lundholm, N.; Thoms, S.; Richter, K.U.; Krock, B.; Hansen, P.J.; Rost, B. Inorganic carbon acquisition in potentially toxic and non-toxic diatoms: The effect of pH-induced changes in seawater carbonate chemistry. *Physiol. Plant.* **2008**, *133*, 92–105. [[CrossRef](#)]
122. Brunson, J.K.; McKinnie, S.M.K.; Chekan, J.R.; McCrow, J.P.; Miles, Z.D.; Bertrand, E.M.; Bielinski, V.A.; Luhavaya, H.; Obornik, M.; Smith, G.J.; et al. Biosynthesis of the neurotoxin domoic acid in a bloom-forming diatom. *Science* **2018**, *361*, 1356–1358. [[CrossRef](#)]
123. Miller, F.J.; Woosley, R.; DiTrollo, B.; Waters, J. Effect of ocean acidification on the speciation of metals in seawater. *Oceanography* **2009**, *22*, 72–85. [[CrossRef](#)]

124. Perez, P.; Beiras, R.; Fernandez, E. Monitoring copper toxicity in natural phytoplankton assemblages: Application of Fast Repetition Rate fluorometry. *Ecotoxicol. Environ. Saf.* **2010**, *73*, 1292–1303. [[CrossRef](#)]
125. Rue, E.; Bruland, K. Domoic acid binds iron and copper: A possible role for the toxin produced by the marine diatom *Pseudo-nitzschia*. *Mar. Chem.* **2001**, *76*, 127–134. [[CrossRef](#)]
126. Lelong, A.; Jolley, D.F.; Soudant, P.; Hegaret, H. Impact of copper exposure on *Pseudo-nitzschia* spp. physiology and domoic acid production. *Aquat. Toxicol.* **2012**, *118–119*, 37–47. [[CrossRef](#)] [[PubMed](#)]
127. Bates, S.S.; Léger, C.; Satchwell, M.; Boyer, G.L. The effects of iron on domoic acid production by *Pseudo-nitzschia* multiseriis. In Proceedings of the 9th International Conference on Harmful Algal Blooms, Hobart, Tasmania, 7–11 February 2000; pp. 320–323.
128. Kobayashi, K.; Takata, Y.; Kodama, M. Direct contact between *Pseudo-nitzschia* multiseriis and bacteria is necessary for the diatom to produce a high level of domoic acid. *Fish. Sci.* **2009**, *75*, 771–776. [[CrossRef](#)]
129. Bates, S.S.; Douglas, D.J.; Doucette, G.J.; Leger, C. Enhancement of domoic acid production by reintroducing bacteria to axenic cultures of the diatom *Pseudo-nitzschia* multiseriis. *Nat. Toxins* **1995**, *3*, 428–435. [[CrossRef](#)]
130. Bates, S.S.; Gaudet, J.; Kaczmarek, I.; Ehrman, J.M. Interaction between bacteria and the domoic-acid-producing diatom *Pseudo-nitzschia* multiseriis (Hasle) Hasle; can bacteria produce domoic acid autonomously? *Harmful Algae* **2004**, *3*, 11–20. [[CrossRef](#)]
131. Maas, E.W.; Law, C.S.; Hall, J.A.; Pickmere, S.; Currie, K.I.; Chang, F.; Voyles, K.M.; Caird, D. Effect of ocean acidification on bacterial abundance, activity and diversity in the Ross Sea, Antarctica. *Aquat. Microb. Ecol.* **2013**, *70*, 1–15. [[CrossRef](#)]
132. Schada von Borzyskowski, L.; Bernhardsgrutter, I.; Erb, T.J. Biochemical unity revisited: Microbial central carbon metabolism holds new discoveries, multi-tasking pathways, and redundancies with a reason. *Biol. Chem.* **2020**, *401*, 1429–1441. [[CrossRef](#)]
133. Dickson, A.G. The carbon dioxide system in seawater: Equilibrium chemistry and measurements. *Guide Best Pract. Ocean. Acidif. Res. Data Report.* **2010**, *1*, 17–40.
134. Gattuso, J.-P.; Lavigne, H. Approaches and software tools to investigate the impact of ocean acidification. *Biogeosciences* **2009**, *6*, 2121–2133. [[CrossRef](#)]
135. Gattuso, J.-P.; Lee, K.; Rost, B.; Schulz, K. Approaches and Tools to Manipulate the Carbonate Chemistry. Publications Office of the European Union: Luxembourg, 2010.
136. Llavera, G.; Figueroa, R.I.; Garces, E.; Berdalet, E. Cell Cycle and Cell Mortality of *Alexandrium Minutum* (Dinophyceae) under Small-Scale Turbulence Conditions 1. *J. Phycol.* **2009**, *45*, 1106–1115. [[CrossRef](#)]
137. Shi, D.; Xu, Y.; Morel, F. Effects of the pH/pCO<sub>2</sub> control method on medium chemistry and phytoplankton growth. *Biogeosciences* **2009**, *6*, 1199–1207. [[CrossRef](#)]
138. Hurd, C.L.; Hepburn, C.D.; Currie, K.I.; Raven, J.A.; Hunter, K.A. Testing the effects of ocean acidification on algal metabolism: Considerations for experimental designs. *J. Phycol.* **2009**, *45*, 1236–1251. [[CrossRef](#)]
139. Rost, B.; Zondervan, I.; Wolf-Gladrow, D. Sensitivity of phytoplankton to future changes in ocean carbonate chemistry: Current knowledge, contradictions and research directions. *Mar. Ecol. Prog. Ser.* **2008**, *373*, 227–237. [[CrossRef](#)]
140. Cornwall, C.E.; Hurd, C.L. Experimental design in ocean acidification research: Problems and solutions. *ICES J. Mar. Sci.* **2016**, *73*, 572–581. [[CrossRef](#)]
141. Fiehn, O. Metabolomics—The link between genotypes and phenotypes. *Plant Mol. Biol.* **2002**, *48*, 155–171. [[CrossRef](#)] [[PubMed](#)]
142. Cho, Y.; Tsuchiya, S.; Omura, T.; Koike, K.; Oikawa, H.; Konoki, K.; Oshima, Y.; Yotsu-Yamashita, M. Metabolomic study of saxitoxin analogues and biosynthetic intermediates in dinoflagellates using (15)N-labelled sodium nitrate as a nitrogen source. *Sci. Rep.* **2019**, *9*, 3460. [[CrossRef](#)]
143. Brown, E.R.; Moore, S.G.; Gaul, D.A.; Kubanek, J. Predator cues target signaling pathways in toxic algal metabolome. *Limnol. Oceanogr.* **2022**, *67*, 1227–1237. [[CrossRef](#)]
144. Jang, C.; Chen, L.; Rabinowitz, J.D. Metabolomics and Isotope Tracing. *Cell* **2018**, *173*, 822–837. [[CrossRef](#)]
145. Rahim, M.; Ragavan, M.; Deja, S.; Merritt, M.E.; Burgess, S.C.; Young, J.D. INCA 2.0: A tool for integrated, dynamic modeling of NMR- and MS-based isotopomer measurements and rigorous metabolic flux analysis. *Metab. Eng.* **2022**, *69*, 275–285. [[CrossRef](#)]
146. Wang, Y.; Wondisford, F.E.; Song, C.; Zhang, T.; Su, X. Metabolic Flux Analysis-Linking Isotope Labeling and Metabolic Fluxes. *Metabolites* **2020**, *10*, 447. [[CrossRef](#)]
147. Treves, H.; Kuken, A.; Arrivault, S.; Ishihara, H.; Hoppe, I.; Erban, A.; Hohne, M.; Moraes, T.A.; Kopka, J.; Szymanski, J.; et al. Carbon flux through photosynthesis and central carbon metabolism show distinct patterns between algae, C(3) and C(4) plants. *Nat. Plants* **2022**, *8*, 78–91. [[CrossRef](#)]
148. Gimenez, I.; Waldbusser, G.G.; Langdon, C.J.; Hales, B.R. The dynamic ocean acidification manipulation experimental system: Separating carbonate variables and simulating natural variability in laboratory flow-through experiments. *Limnol. Oceanogr. Methods* **2019**, *17*, 343–361. [[CrossRef](#)]
149. West, J.J.; Järnberg, L.; Berdalet, E.; Cusack, C. Understanding and Managing Harmful Algal Bloom Risks in a Changing Climate: Lessons From the European CoCliME Project. *Front. Clim.* **2021**, *3*. [[CrossRef](#)]
150. Kremp, A.; Godhe, A.; Egardt, J.; Dupont, S.; Suikkanen, S.; Casabianca, S.; Penna, A. Intraspecific variability in the response of bloom-forming marine microalgae to changed climate conditions. *Ecol. Evol.* **2012**, *2*, 1195–1207. [[CrossRef](#)] [[PubMed](#)]
151. Anderson, D.M.; Andersen, P.; Bricelj, V.M.; Cullen, J.J.; Rensel, J.J. *Monitoring and Management Strategies for Harmful Algal Blooms in Coastal Waters*; UNESCO: Paris, France, 2001.

152. Anderson, C.R.; Kudela, R.M.; Kahru, M.; Chao, Y.; Rosenfeld, L.K.; Bahr, F.L.; Anderson, D.M.; Norris, T.A. Initial skill assessment of the California Harmful Algae Risk Mapping (C-HARM) system. *Harmful Algae* **2016**, *59*, 1–18. [[CrossRef](#)] [[PubMed](#)]
153. Davidson, K.; Anderson, D.M.; Mateus, M.; Reguera, B.; Silke, J.; Sourisseau, M.; Maguire, J. Forecasting the risk of harmful algal blooms. *Harmful Algae* **2016**, *53*, 1–7. [[CrossRef](#)] [[PubMed](#)]

**Disclaimer/Publisher’s Note:** The statements, opinions and data contained in all publications are solely those of the individual author(s) and contributor(s) and not of MDPI and/or the editor(s). MDPI and/or the editor(s) disclaim responsibility for any injury to people or property resulting from any ideas, methods, instructions or products referred to in the content.